JOURNAL OF THE

Electrochemical Society

Engineering Library

LIBRARY UNIVERSITY OF UTAH JAN 30 1950 SALT LAKE CITY

Vol. 97, No. 1 January, 1950

Published Monthly by

THE ELECTROCHEMICAL SOCIETY

LIBRARY
UNIVERSITY OF UTAH

Journal of the

Electrochemical Society

JANUARY 1950 VOLUME 97 • NUMBER 1

CONTENTS

Effect of Adsorbed Polar Organic Compounds on Activity of Steel in Acid Solution. *N. Hackerman and E. L. Cook* 1

The Electrochemical Behavior of Aluminum, I. In Solutions of Cerium Sulfate in Sulfuric Acid. *J. V. Petrocelli* 10

Polarographic Investigation of Mercaptobenzothiazole. *G. Sartori and A. Liberti* 20

Effect of Thermal History on Color of Zinc Beryllium Silicate (Mn) Phosphors. *S. Jones* 25

Ultraviolet Emitting Phosphor. *R. Nagy, et al.* 29

Zinc Sulfide Infrared Quenching Phosphors. *N. T. Melamed* 33

Technical Reviews

Review of Articles on Luminescence for 1949. *G. R. Fonda* 3C

Developments of Germanium and Gallium during 1949. *J. R. Musgrave* 8C

Feature Section

Research in Industry—Is Government Antagonistic to It? *O. W. Storey* 9C

Current Affairs

Cleveland Convention Plans 18C

Activities of the Rare Metals Group for 1949 ..... 19C

Candidates for Office 20C

Meeting of ASA and A. I. Ch. E. 21C

Corrosion Research Forum 22C

Section News 22C

Personals 24C

New Members 24C

New Publications 25C

Recent Patents 26C

Future Meetings of Other Organizations 27C

Employment Situations 27C

H. H. Uhlig, *Editor*

H. J. Read, *Technical Editor* — F. L. LaQue, *Business Manager* — R. M. Burns, *Consultant*

Eleanor Reid, *Managing Editor* — H. B. Linford, *Associate Editor* — U. B. Thomas, *Associate Editor* — R. G. Ellis, *Advertising Manager*

Divisional Representatives

J. M. Bialosky — Paul S. Brallier — N. C. Cahoon — C. L. Faust — H. C. Froelich

A. E. Pavlish — E. B. Sanigar — Sherlock Swann, Jr. — Archie J. Weith

Published monthly by The Electrochemical Society, Inc., Mt. Royal and Guilford Aves., Baltimore 2, Md., combining the Journal and Transactions of The Electrochemical Society. Editorial Office: 235 W. 102nd St., New York 25, N. Y. Statements and opinions given in articles and papers in the Journal of The Electrochemical Society are those of the contributors, and The Electrochemical Society assumes no responsibility for them. Subscription: $7.50 to members, $10.00 to nonmembers. Single copies $.75 to members, $1.00 to nonmembers. Copyright 1950 by The Electrochemical Society. Entered as second-class matter November 15, 1947, at the Post Office at Baltimore, Md., under the act of August 24, 1912.

Effect of Adsorbed Polar Organic Compounds on Activity of Steel in Acid Solution[1, 2]

NORMAN HACKERMAN AND E. L. COOK[3]

Department of Chemistry, The University of Texas, Austin, Texas

ABSTRACT

A series of aliphatic acids, amines, and esters, as well as one commercial corrosion inhibitor, were adsorbed from benzene solution onto SAE 1020 steel powder. These studies (reported elsewhere) showed that some portion of the sorbed material, depending on the compound, could not be desorbed by fresh solvent. The present work was concerned with the effect of the adsorbed material on the activity of the steel powder in aqueous HCl. Dual adsorptions, e.g., an acid followed by an amine on the same steel sample, were also carried out and activities of the metal so treated were determined. The ratio of the activity to that of untreated steel powder, the relative activity, was found to depend on the compound adsorbed and on the type of adsorption. The order of inhibitor effectiveness was about the same as the order of adsorption from benzene, both reversible and irreversible. In general, the acids and amines were considerably more effective as inhibitors than the alcohols and esters. For the acid, amine, and alcohol series, the C_{18} compounds showed optimum effectiveness. When two inhibitors are used in the same system, greater inhibition is obtained if each adsorbs on different areas.

INTRODUCTION

The inhibition of metal corrosion has been studied by numerous investigators for obvious practical reasons. The methods of approach in such studies have also been widespread. Rhodes and Kuhn (1) observed the inhibiting character of acridine and its derivatives by measuring the rate of hydrogen evolution given off as iron wire dissolved in inhibited 1*N* H_2SO_4. The higher molecular weight derivatives of the same series generally were found to be better inhibitors against acid attack. An attempt to relate quantitatively the protective character of the adsorbed film with the ohmic resistance of the film was not successful although qualitative relationships were apparent. Mann, Lauer, and Hultin (2) demonstrated the inhibitive character of mono-, di-, and tri-alkyl amines containing from one to five carbon atoms in the alkyl group. By measuring the loss in weight of a mild steel sample immersed in 1*N* H_2SO_4 solution containing the inhibitor, they found that both increasing the number of substituent radicals and increasing the chain length of the radical improved the effectiveness of the inhibitor.

Pilz and Farley (3) made a study of rust preventive oils and developed correlations of contact angle of the oil with the surface to be protected as a function of effectiveness of the oil as an inhibitor. Atkins, Baker, Murphy, and Zisman (4) made comparative tests on the suitability of rust preventives in certain synthetic lubricating oils. Baker and Zisman (5) made a comprehensive study and review of polar type rust inhibitors. In general, the better inhibitors were shown to be adsorbed from the oil phase by the metal to such an extent that moisture was displaced from the metal surface, or moisture penetration through the adsorbed inhibitor film was minimized.

Inasmuch as the corrosion process takes place at the metal-medium interface, the present study was approached as a problem in adsorption. To permit a more detailed study of the individual operating variables, adsorption of polar organic compounds from benzene solution was considered in another study (6) whereas, in the subject investigation, the inhibitive character of the adsorbed compounds in aqueous acid media was undertaken.

Hackerman and Cook (6) showed that n-alkyl

[1] Manuscript received June 20, 1949. This paper prepared for delivery before the Chicago Meeting, October 12 to 15, 1949.

[2] Based in part on a thesis submitted by E. L. Cook to the Graduate School of the University of Texas in partial fulfillment of the requirements for the Ph.D. degree.

[3] Present address: Magnolia Petroleum Company, Field Research Laboratory, Dallas, Texas.

277183

acids, amines, alcohols, and certain esters with chain lengths varying from 10 to 18 carbon atoms were adsorbed from benzene solution on 1020 steel powder. Further, all of the adsorption was not reversible, the amount of irreversible adsorption being dependent on the functional group. Fig. 1 shows adsorption and desorption isotherms, respectively, for the 18 carbon atom compound of each homologous series studied. Total adsorption, reversible plus irreversible, was found to be greater with the longer chain length, but the irreversible portion was independent of chain length. The amount of total adsorption and irreversible adsorption for the same chain length was in the order acids > amines > alcohols > esters. It was

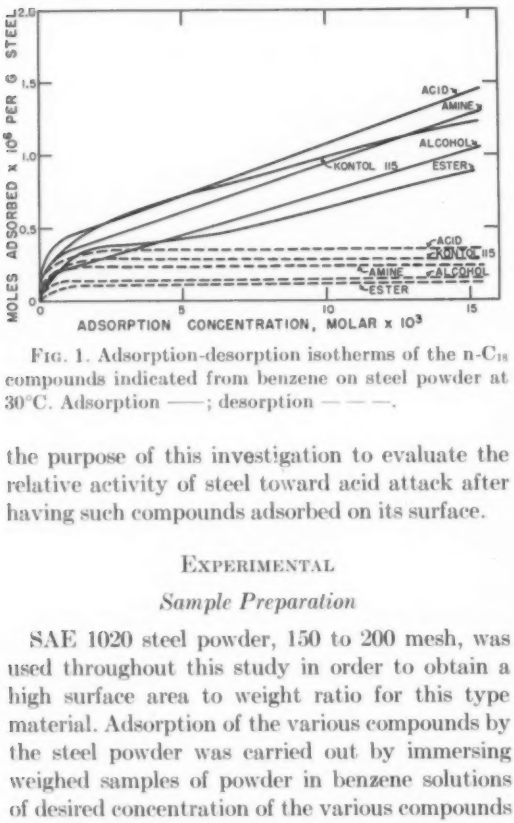

FIG. 1. Adsorption-desorption isotherms of the n-C_{18} compounds indicated from benzene on steel powder at 30°C. Adsorption ——; desorption — — —.

the purpose of this investigation to evaluate the relative activity of steel toward acid attack after having such compounds adsorbed on its surface.

EXPERIMENTAL

Sample Preparation

SAE 1020 steel powder, 150 to 200 mesh, was used throughout this study in order to obtain a high surface area to weight ratio for this type material. Adsorption of the various compounds by the steel powder was carried out by immersing weighed samples of powder in benzene solutions of desired concentration of the various compounds to be studied. The adsorption concentrations varied from 0.375×10^{-3} to 15×10^{-3} molar. The amount of adsorption was determined gravimetrically by noting the weight increase of the steel powder due to the adsorbed compound. The amount of irreversible adsorption was determined by repeatedly contacting the powder with the adsorbed component with pure benzene until no further desorption took place. The amount of undesorbed component was again determined directly by gravimetric means. Complete details of the adsorption and desorption procedure, apparatus, and materials used have been described elsewhere (6).

Samples of steel powder used in the subject investigation were portions of the samples used in the adsorption experiments. The compounds which were adsorbed by the steel were the alkyl acids varying in chain length from 6 to 18 carbon atoms, the alkyl amines from 8 to 18 carbon atoms, and the alcohols from 10 to 18 carbon atoms. Methyl, ethyl, and n-butyl stearate, and ethyl laurate were also studied. The acids except caproic and benzoic were cp grade obtained from the Paragon Testing Laboratories. Melting points and freezing points deviated not more than 1.0°C from the values reported by Mumford and Phillips (7). The caproic and benzoic acids were cp grades obtained from Bender and Hobein, Munich, Germany, and Baker Chemical Company. The alcohols were Eastman best grade and the esters were cp grade obtained from Paragon. The amines were of the "distilled" grades, all being of 90 per cent purity or better, the impurities being amines containing 2 CH_2 groups more or less than the subject compound. A commercial inhibitor, Kontol 115,[1] used successfully in inhibiting natural gas wells, was also studied.

Relative Acidity Test

The protective character of the adsorbed polar compounds against acid attack was indicated by the rate with which the metal dissolved in acid solution and liberated hydrogen gas. The test which was used throughout this study required the use of 5 grams (±1 mg) of the dry metal powder upon which the given compound was adsorbed. The weighed sample was placed in a 250 ml Erlenmeyer flask to which a gas delivery tube and a 100 ml burette were connected by means of a rubber stopper. The discharge tube led to an inverted water-filled graduated cylinder. The flask and graduated cylinders were partially immersed in a water bath maintained at 30°C (±0.1°C). By means of the burette, 100 ml of 4.00*N* HCl were measured into the Erlenmeyer flask and the hydrogen evolved as a result of the acid attack on

[1] Kindly supplied by the Tretolite Company, St. Louis, Missouri.

the steel observed in the graduated cylinder. A 100 ml correction was made for the volume of air displaced by the acid.

The time required for the production of 36, 81, and 126 ml of hydrogen gas was recorded, the starting time being taken at the instant the first drop of acid was discharged from the burette. Since 100 ml of 4.00*N* acid represented a 100 per cent excess over the amount required to completely dissolve the steel, and the quantities of hydrogen evolved represented only 1.6, 3.4, and 5.2 per cent of the metal being dissolved, a maximum decrease in concentration of the acid from 4.00 to 3.90*N* occurred during the test period, thereby causing only a very slight change in the rate of attack due to concentration changes.

The effectiveness of the polar compound on the steel powder as an inhibitor was indicated by comparing the time for evolving the above given quantities of hydrogen to that for a similar sample of fresh steel powder which had no adsorbed polar compound on its surface. The ratio of the period for the untreated powder to the respective period for the treated powder was taken as the *relative activity*.

The duplicability of this test was within ±5 per cent. By assuming a surface area of 0.07 m^2/g for the steel powder, based on a minimum value obtained from adsorption data, the data expressed as relative activity may be converted to corrosion units of mdd by multiplying the initial relative activity by a factor of 366.

Results and Discussion

Acids

Fig. 2, 3, and 4 show the relative activity data for stearic, capric, and caproic acids, respectively, plotted against the concentration of the various solutes when adsorbed from benzene solution. The relative activity of the metal toward acid attack during the dissolution of the first increment of the metal (0–1.6% by weight) gave a curve similar to an adsorption isotherm when plotted against the adsorption concentration. However, comparison of the relative activity curves with the adsorption curves indicates the greater adsorption at the higher concentrations did not materially decrease the relative activity further. After 1.6 per cent of the metal had dissolved, however, the relative activity in the lower adsorption concentrations increased markedly, whereas the higher concentrations increased only slightly. After 3.4 per cent of the metal had dissolved, a further slight increase occurred. This was noted throughout the concentration range studied.

Each figure also shows results obtained on samples after they had been subjected to the benzene desorption procedure. Relative activities of the desorbed samples also gave an adsorption isotherm type curve when the initial relative activities were plotted against the original adsorption concentration. The flat type curve was similar to the adsorption isotherm for the desorbed samples and the displacement of the curve from unity may be attributed entirely to the undesorbed portion observed in the desorption studies. After dissolution of 1.6 per cent of the metal, however, the relative activity approached 1.0 at all adsorption concentrations. It is of interest to note that the activity exceeded 1.0 at the most dilute adsorption concentrations. This dip in the curve cannot be attributed to experimental error and was observed in numerous cases. The alcohols and esters showed this effect most strongly, acids and amines showing it to a lesser extent.

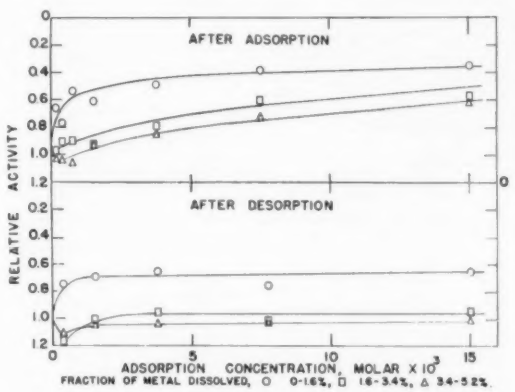

Fig. 2. Relative activity curves for steel pretreated with stearic acid as indicated. The activity of untreated steel powder is taken as unity on all of the relative activity curves.

A possible explanation of the "promoter action" is that a portion of the adsorbed polar molecules are desorbed by the medium or blown off the surface by evolving hydrogen. These molecules lower the interfacial tension of the aqueous medium surrounding the metal particle. As a bubble of hydrogen gas is formed on the surface of the metal particle, a liquid-gas interface forms, for which there is a certain contact angle on the

metal. If the interfacial tension is further decreased, the contact angle through the liquid with the metal surface will be decreased and the bubble will be displaced more readily than if the interfacial tension had not been reduced. The observed promoter action is, therefore, believed to be due to the reduction in the number of big hydrogen bubbles present on the surface of the particles as a result of the interfacial tension lowering.

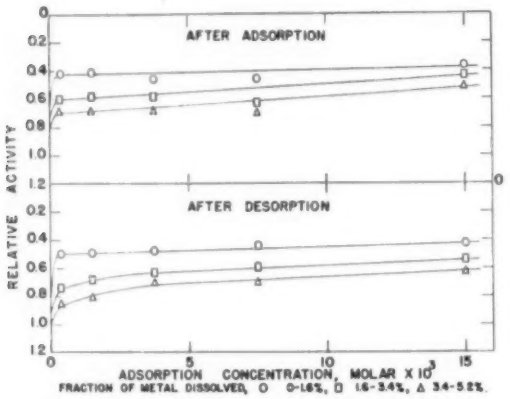
AFTER ADSORPTION
AFTER DESORPTION
RELATIVE ACTIVITY
ADSORPTION CONCENTRATION, MOLAR X 10³
FRACTION OF METAL DISSOLVED, O 0-1.6%, □ 1.6-3.4%, Δ 3.4-5.2%

FIG. 3. Relative activity curves; capric acid

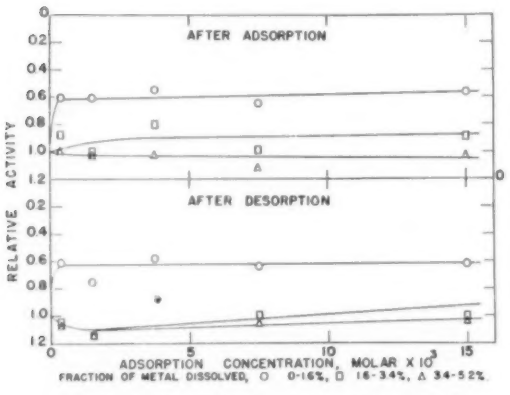
AFTER ADSORPTION
AFTER DESORPTION
RELATIVE ACTIVITY
ADSORPTION CONCENTRATION, MOLAR X 10³
FRACTION OF METAL DISSOLVED, O 0-1.6%, □ 1.6-3.4%, Δ 3.4-5.2%

FIG. 4. Relative activity curves; caproic acid

New bubbles formed on the same points would not be as large. This implies that the true rate of acid attack is not accelerated, but that the apparent rate of hydrogen evolution is affected by the change in hydrogen inventory on the surface. Once the solution reaches a near equilibrium interfacial tension, the steady state evolution rate is realized. Further work on this aspect is anticipated.

Capric acid data are shown in Fig. 3. It should be noted that not only is the initial activity level slightly lower in value than stearic acid, but that subsequent dissolution did not increase the activity value markedly. Further, after desorption of the steel samples, the relative activity values increased only slightly over the original samples. This indicates that the undesorbed portion of the C_{10} acid was responsible for the major portion of the reduction in rate of acid attack on the steel, contrary to the action of stearic acid. Palmitic and lauric acids are not shown, but their inhibiting characteristics fell between those described here for stearic and capric acids.

As previously described (6), caproic acid sorption from benzene solution on steel was so strong that complete reaction with the metal was observed as indicated by the blue coloration of the adsorption solutions due to ferrous caproate. However, the extent of metal dissolution due to the caproic acid attack was small. Desorption experiments indicated the principal portion of the adsorbed phase to be undesorbable. The relative activity data for caproic acid samples, shown in Fig. 4, confirm such observations. The initial relative activities of the adsorbed and desorbed samples were essentially the same. The inhibitive action of caproic acid was notably inferior to either stearic or capric acids. After 1.6 per cent of the metal had dissolved, no protective action was apparent and data obtained on such samples were erratic.

Benzoic acid attacked the steel powder strongly, even in benzene solution (6). Relative activity data (not shown) indicated that neither the adsorbed nor the desorbed samples were inhibited to any appreciable extent.

Amines

Fig. 5, 6, and 7 show the relative activity of steel samples with adsorbed octadecyl, decyl, and octyl amines, respectively. Hexadecyl, tetradecyl, and dodecyl amines were also studied, but showed no unusual behavior. Octadecyl amine was not as effective as the corresponding acid in reducing the activity of the metal against acid attack. The desorbed samples were particularly ineffective. Decyl amine, however, gave results similar to those for capric acid. The adsorbed samples continued to show good inhibition even after 5.2 per cent of the metal was dissolved. Desorption did not increase the initial activity of the metal appreciably, but after 1.6 per cent dissolution the rate

increased more rapidly than with the adsorbed samples.

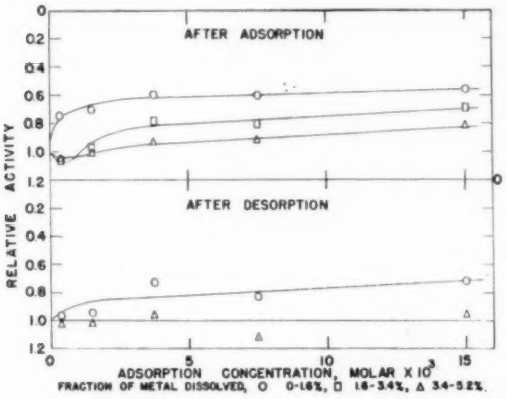
AFTER ADSORPTION
AFTER DESORPTION
RELATIVE ACTIVITY
ADSORPTION CONCENTRATION, MOLAR X 10³
FRACTION OF METAL DISSOLVED, O 0-16%, □ 16-34%, Δ 34-52%.

FIG. 5. Relative activity curves; octadecyl amine

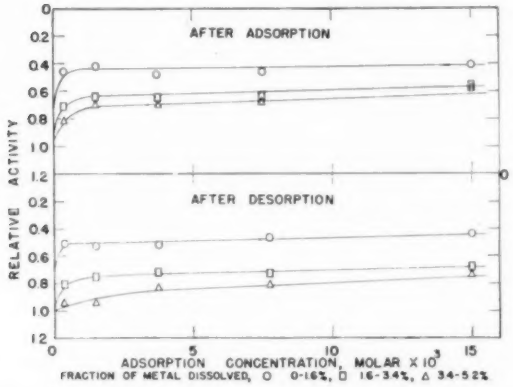
AFTER ADSORPTION
AFTER DESORPTION
RELATIVE ACTIVITY
ADSORPTION CONCENTRATION, MOLAR X 10³
FRACTION OF METAL DISSOLVED, O 0-16%, □ 16-34%, Δ 34-52%

FIG. 6. Relative activity curves; decyl amine

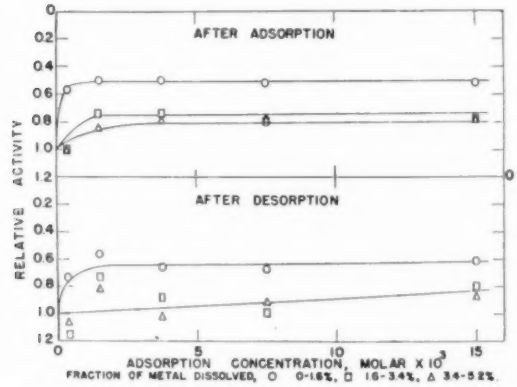
AFTER ADSORPTION
AFTER DESORPTION
RELATIVE ACTIVITY
ADSORPTION CONCENTRATION, MOLAR X 10³
FRACTION OF METAL DISSOLVED, O 0-16%, □ 16-34%, Δ 34-52%

FIG. 7. Relative activity curves; octyl amine

Samples with adsorbed octyl amine were inferior to decyl amine samples in that the initial activities were much higher and continued dissolution of the metal caused rapid increase in the rate of acid attack. Desorption of octyl amine increased the activity markedly. It should be pointed out that the C_{10} amine, like the C_{10} acid, appeared to give the best inhibition against acid attack. This appeared to be true particularly for the desorbed samples, although the amount of irreversibly adsorbed component, on a moles/unit area basis, was essentially the same for each homologous series. Tetradecyl and dodecyl amine samples (curves not shown here) gave slightly lower initial activities than decyl amine at the highest adsorption concentrations but, as dissolution progressed, the rates increased more than for samples with adsorbed decyl amine. The desorbed C_{14} and C_{12} amine samples were not as effectively inhibited as the desorbed C_{10} amine samples.

Alcohols

Fig. 8 and 9 show the relative activity data obtained on samples with adsorbed octadecyl and decyl alcohols, respectively. The alcohols, as a group, were less effective than acids or amines in reducing the rate of acid attack. After the first increment of dissolution, it is to be noted that the apparent rate of acid attack increased to give a relative activity in excess of 1.0. This phenomenon, ascribed to lowering of the interfacial tension, was described above in connection with the organic acids. The alcohols showed this effect more than any of the other homologous series studied. Desorption of octadecyl alcohol left the steel surface inhibited only to a very slight extent, and after the first increment of dissolution, the rate of attack went through a maximum and then approached that of the uninhibited metal.

The relative activity in excess of 1.0 is again explained on the basis of a decrease in inventory of hydrogen gas adsorbed on the metal surface due to the lowering of the interfacial tension. Decyl alcohol gave results similar to those for octadecyl alcohol in most respects, except that the relative activity remained considerably lower after the first increment was dissolved. Desorption increased the initial activity only slightly, but subsequent dissolution was apparently "promoted" due to the interfacial tension lowering. Cetyl, myristyl, and lauryl alcohols were also run but differed only in that samples with adsorbed cetyl and myristyl alcohols gave slightly lower initial activities than decyl alcohol. Either subsequent dissolution of the metal or desorption increased the

relative activity to values above those of decyl alcohol.

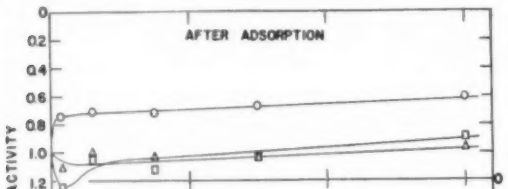
AFTER ADSORPTION
AFTER DESORPTION
RELATIVE ACTIVITY
ADSORPTION CONCENTRATION, MOLAR X 10³
FRACTION OF METAL DISSOLVED, O 0-1.6%, □ 1.6-3.4%, Δ 3.4-5.2%

FIG. 8. Relative activity curves; octadecyl alcohol

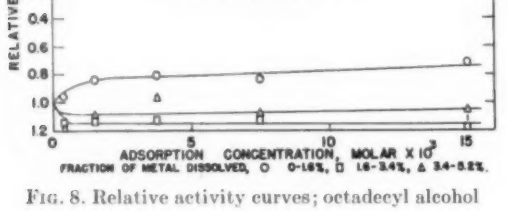
AFTER ADSORPTION
AFTER DESORPTION
RELATIVE ACTIVITY
ADSORPTION CONCENTRATION, MOLAR X 10³
FRACTION OF METAL DISSOLVED, O 0-1.6%, □ 1.6-3.4%, Δ 3.4-5.2%

FIG. 9. Relative activity curves; decyl alcohol

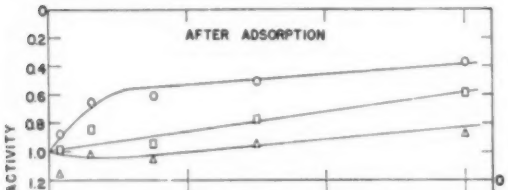
AFTER ADSORPTION
AFTER DESORPTION
RELATIVE ACTIVITY
ADSORPTION CONCENTRATION, MOLAR X 10³
FRACTION OF METAL DISSOLVED, O 0-1.6%, □ 1.6-3.4%, Δ 3.4-5.2%

FIG. 10. Relative activity curves; methyl stearate

Esters

Relative activity data on samples with adsorbed methyl stearate are shown in Fig. 10. Ethyl and butyl stearate and butyl laurate were also studied, but gave similar results and are not shown. The adsorbed samples were initially effective in lowering the activity but subsequent dissolution caused increased activity, particularly for the samples where adsorption took place in the lower concentrations. The esters also displayed the apparent promoting effect to some extent. Increasing the size of the alcohol group of the ester from one to four carbon atoms had no appreciable effect on inhibitive properties of the ester, nor did decreasing the length of the acid chain from 18 to 12 carbon atoms.

Commercial Inhibitor

Relative activity data obtained on Kontol 115, a commercial inhibitor, are shown in Fig. 11. The

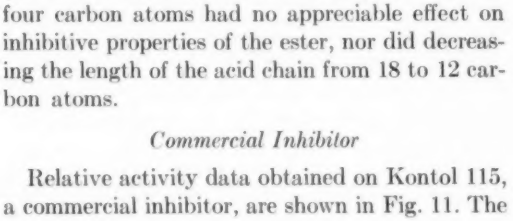
AFTER ADSORPTION
AFTER DESORPTION
RELATIVE ACTIVITY
ADSORPTION CONCENTRATION, MOLAR X 10³
FRACTION OF METAL DISSOLVED, O 0-1.6%, □ 1.6-3.4%, Δ 3.4-5.2%

FIG. 11. Relative activity curves; Kontol 115

isotherms (Fig. 1) for this compound (a n-alkyl succinimide with a molecular weight of approximately 350) are typical of those obtained with the various alkyl homologous series described formerly (6). The relative activity data are similar to those obtained from the acids and amines. The adsorbed samples showed low initial activities which increased slowly with continued dissolution. Desorption increased the initial activity only slightly although subsequent dissolution brought about a more rapid increase in activity.

Dual Adsorbed Systems

During the course of adsorption studies with the steel powder-benzene-solute system (8), it was found that the steel samples with irreversibly adsorbed acid, when placed in benzene solutions of amines, adsorbed the amine without apparent loss or displacement of the originally irreversibly ad-

sorbed acid. The amount of irreversibly adsorbed amine was less than the amount of irreversibly adsorbed amine normally taken up by fresh steel samples, although the reversible portion was only slightly less than that obtained with fresh powder.

The reverse system, first adsorption of amine, desorption, and adsorption of acid along with the undesorbable amine, gave similar results.

The adsorption of acid on steel samples, which had undergone the adsorption-desorption cycle with either alcohol or ester, behaved in a similar manner except the quantity of irreversibly adsorbed acid taken up, plus the already present undesorbable alcohol or ester, amounted to that required to cover approximately the same area that the acid alone covered on a fresh steel surface. If, however, acid were first adsorbed, and then adsorption of alcohol or ester permitted, no further increase in the amount of irreversible adsorption was observed. This series of experiments indicated that: (*a*) irreversible adsorption of acids and amines took place to a large extent on different portions of the surface area, but some areas could accommodate either acid or amine; (*b*) alcohols and esters were irreversibly adsorbed on some of the sites on which acids were normally adsorbed and on no others; (*c*) irreversibly adsorbed acids did not displace similarly adsorbed amines or vice versa; (*d*) alcohols and esters, which were irreversibly adsorbed on fresh steel to a lesser extent than were acids, were not irreversibly adsorbed on steel surfaces already holding irreversibly adsorbed acid. Irreversible adsorption of acids on steel with alcohols or esters already irreversibly adsorbed took place only to the extent required to cover the remaining acid adsorbing areas not covered by the alcohol or ester.

Fig. 12 shows the relative activity data on samples which first adsorbed stearic acid, then were desorbed and permitted to adsorb octadecyl amine. The data shown as "desorbed" refer to the samples after desorption of desorbable amine, thereby leaving undesorbable acid and amine on the surface of the steel samples. This system showed the adsorbed samples followed the trends for octadecyl amine (Fig. 5), but the activity level was about 0.15 unit less. The desorbed samples followed that for the desorbed stearic acid (Fig. 2) with the same 0.15 unit decrease in relative activity. The difference, in the first case, may be considered due to the irreversibly adsorbed acid and, in the second case, due to the undesorbable amine.

The dual system, adsorption of lauric acid then desorption followed by adsorption of dodecyl amine, also behaved as described just above with the exception that considerably more inhibition was indicated than with the C_{18} system.

Reversal of the dual adsorption process did not improve the inhibition. Fig. 13 shows the system which first adsorbed octadecyl amine and then stearic acid. The adsorbed samples showed poorer inhibition than stearic acid alone, but were comparable to octadecyl amine alone. The desorbed samples were slightly lower in activity than the desorbed acid samples. The dodecyl amine-lauric acid system followed similar trends.

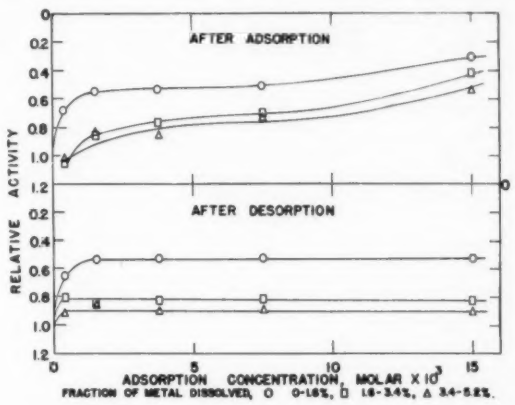
AFTER ADSORPTION
AFTER DESORPTION
RELATIVE ACTIVITY
ADSORPTION CONCENTRATION, MOLAR X 10³
FRACTION OF METAL DISSOLVED, O 0-1.6%, □ 1.6-3.4%, △ 3.4-5.2%.

FIG. 12. Relative activity curves for the dual adsorbed system: stearic acid-octadecyl amine.

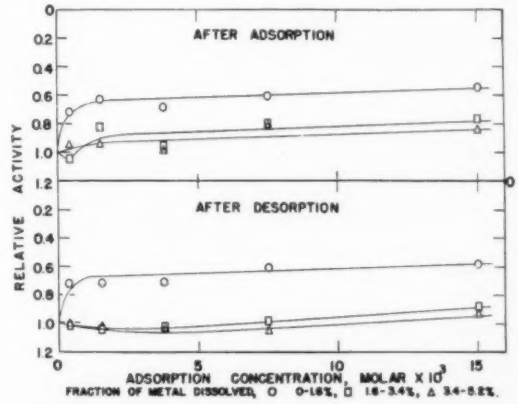
AFTER ADSORPTION
AFTER DESORPTION
RELATIVE ACTIVITY
ADSORPTION CONCENTRATION, MOLAR X 10³
FRACTION OF METAL DISSOLVED, O 0-1.6%, □ 1.6-3.4%, △ 3.4-5.2%.

FIG. 13. Relative activity curves; octadecyl amine-stearic acid.

The stearic acid-octadecyl alcohol system shown in Fig. 14 acted as might have been predicted. The alcohol, adsorbed along with the firmly adsorbed stearic acid, showed an activity level below stearic acid alone, but above octadecyl alcohol. The second dissolution increment displayed

the promoting effect, as did the alcohol samples. The desorbed samples gave activities almost within experimental limits identical with desorbed stearic acid values. This would have been predicted since no alcohol remained adsorbed after the final step in the treatment of samples upon which stearic acid was first adsorbed. The reverse system, shown in Fig. 15, gave results similar to

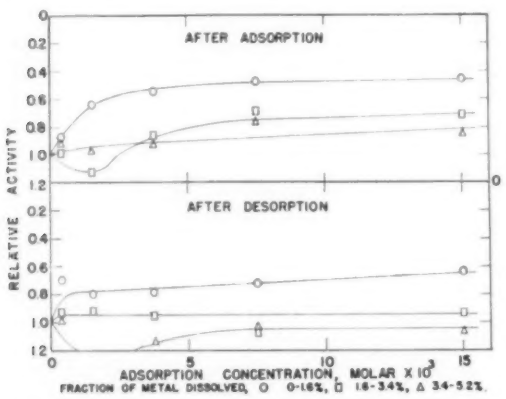
AFTER ADSORPTION
AFTER DESORPTION
RELATIVE ACTIVITY
ADSORPTION CONCENTRATION, MOLAR X 10³
FRACTION OF METAL DISSOLVED, O 0-1.6%, □ 1.6-3.4%, Δ 3.4-5.2%

FIG. 14. Relative activity curves; stearic acid-octadecyl alcohol.

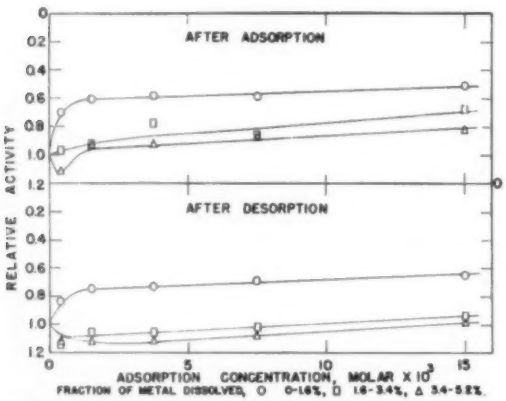
AFTER ADSORPTION
AFTER DESORPTION
RELATIVE ACTIVITY
ADSORPTION CONCENTRATION, MOLAR X 10³
FRACTION OF METAL DISSOLVED, O 0-1.6%, □ 1.6-3.4%, Δ 3.4-5.2%

FIG. 15. Relative activity curves; octadecyl alcohol-stearic acid.

the stearic acid samples. The activity level was slightly higher, probably because of the portion of firmly adsorbed alcohol being inferior to a comparable amount of firmly adsorbed acid in reducing the activity. The desorbed samples showed activities only slightly higher than for stearic acid. This indicated again that the presence of the firmly adsorbed alcohol was inferior to an equivalent amount of acid.

The stearic acid-methyl stearate and reverse systems gave essentially the same results as the acid-alcohol systems, the ester taking the part of the alcohol.

CONCLUSIONS

It was found, in the systems used in this study, that acids and amines were considerably better inhibitors than alcohols and esters. This order is the same as the extent of total adsorption or irreversible adsorption from benzene solution by the steel. Adsorption from solutions of high concentrations did not improve the initial protecting ability of the compounds to any marked extent, but under prolonged acid attack, the inhibition lasted longer. The flat nature of the activity vs. adsorption concentration curves indicates that the total amount of polylayer, or less firm adsorption, is not initially as effective as the irreversible adsorption, but apparently becomes effective as dissolution of the metal continues. This may be explained by migration of loosely adsorbed molecules onto areas where corrosion or hydrogen evolution brings about fresh uncovered surface.

The alcohols, in particular, appeared to act as promoters for a short period after an initial period of inhibition. This was probably only an apparent promotion which was brought about by a change in size of the hydrogen bubbles evolved. Since the corrosion rate was indicated by the hydrogen evolution rate, a decrease in the interfacial tension of the surrounding solution decreased the amount of hydrogen gas adsorbed on the surface. During such a period of change in inventory of gas on the surface, an anomalous corrosion rate would result.

With the acids, amines, and alcohols, the C_{18} compound showed the best inhibiting properties. Chain lengths of more or less than 10 carbon atoms were comparatively less effective. This was particularly true of the samples which had been desorbed. Apparently this chain length is optimum for the combination of forces required of a good inhibitor. It should be noted from adsorption studies (6) that the amount adsorbed is not a maximum at this chain length for any of the homologous series studied.

The function of an inhibitor may be broadly considered as twofold: (*a*) The molecules should form a barrier to prevent diffusion of the corrosive agent to and the corrosion products from the surface. This is performed both by properly oriented chains and functional groups. A longer chain would

presumably improve this property. (*b*) The activity of the metal in the surface should be decreased by bonding with the irreversibly adsorbed component. The better inhibition shown by the C_{10} compound is considered to be due to the enhanced activity of the functional group as compared to the longer chain compound. Thus, by using a longer chain than the above indicated optimum of C_{10} with a more active functional group, or with an activating influence such as an α-substitution, a better inhibitor would result. The activity of the functional group must not be great enough to cause complete reaction with the metal.

The use of more than one inhibitor in systems similar to those used in this work is more effective when the two components are capable of being adsorbed on different specific areas.

Acknowledgment

This work was carried out as a part of Contract N5ori-136, T. O. II with the Office of Naval Research. The authors wish to take this opportunity to express their appreciation to the Office of Naval Research for their support.

Any discussion of this paper will appear in a Discussion Section, to be published in The December 1950 issue of the Journal.

References

1. F. H. Rhodes and W. E. Kuhn, *Ind. Eng. Chem.*, **21,** 1066 (1929).
2. C. A. Mann, B. P. Lauer, and C. T. Hultin, *Ind. Eng. Chem.*, **28,** 159 (1936).
3. G. P. Pilz and F. F. Farley, *Ind. Eng. Chem.*, **38,** 601 (1946).
4. D. C. Atkins, H. R. Baker, C. M. Murphy, and W. A. Zisman, *Ind. Eng. Chem.*, **39,** 491 (1947).
5. H. R. Baker and W. A. Zisman, *Ind. Eng. Chem.*, **40,** 2338 (1948).
6. Norman Hackerman and E. L. Cook, To be published.
7. S. A. Mumford and J. W. C. Phillips, *Rec. trav. chim.*, **52,** 176 (1933).
8. E. L. Cook and Norman Hackerman, To be published.

The Electrochemical Behavior of Aluminum

I. In Solutions of Cerium Sulfate in Sulfuric Acid[1]

J. V. Petrocelli

The Patent Button Company, Waterbury, Connecticut

ABSTRACT

A study has been made of the reactivity of pure aluminum with cerium^{+4} sulfate in sulfuric acid. Electrode potentials, weight loss data, and polarization curves are presented, and it is shown that the reaction may be interpreted from an electrochemical point of view. The theory of the "mixed potential" is suggested as a more generalized concept than the local cell idea for the interpretation of the dissolution process. A brief outline of a probable mechanism for the dissolution and passive behavior of aluminum is presented.

Introduction

The reaction of metals with electrolytes has been a subject of rather intensive study for many years, and although a wealth of experimental data has been accumulated, there are many details concerning the reaction mechanism which are still unknown or obscure (1). Many of the theories which have been proposed to explain some of the important phenomena concerned in the reaction such as hydrogen overvoltage and passivity are not generally acceptable (2, 3). The electrochemical theory of corrosion which postulates local cell action on the metal surface has, however, gained a wide popularity, if not a general acceptance. But even here, many questions arise as to the exact nature of the local cathodic and anodic areas (4, 5).

The work reported in this paper is part of an investigation which is aimed at obtaining some basic information on the mechanism of electrode reactions. Aluminum was chosen for the following reasons: (*a*) it can be obtained in a relatively pure state; (*b*) although from a thermodynamic point of view it should be very reactive with most all electrolytes, it reacts very slowly and exhibits electrode potentials which are quite noble to its reversible potential; (*c*) it shows, under many conditions, rectifying properties. It was also decided that some oxidation-reduction system which has a fairly noble standard potential would be an interesting substance to use as the electron acceptor. With such a system, the cathodic portion of the reaction should be fairly well defined within some characteristic voltage and current range. The work with the system cerium^{+4}-cerium^{+3} sulfate in sulfuric acid is reported here.

The standard electrode potential of this system and the fact that the cerium^{+4} ion forms a complex has been determined by Smith and Getz (8). The characteristics of the polarization curves for the system on inert electrodes have been determined in this laboratory (9).

Mixed Potential Theory and Nomenclature

Generally, when a reaction takes place between a metal and an electrolyte, it may be interpreted in terms of current flow across the metal-solution interface. According to the modern theory of solids (10), a metal is composed of positively charged ions situated at the lattice points, while the valence electrons are quasi-free forming a sort of electron gas which obeys the Fermi-Dirac statistics. These electrons are not bound to any particular ion but move rapidly through the metal in such a way as to maintain an approximate uniform density.

In any reaction, therefore, we may consider the reacting components of the metallic phase to be the positive ions and electrons which make transitions across the metal-solution interface. The current carried by the positive ions when they leave the metal lattice and go into the solution may be considered as an anodic current, i_a, and the current carried by the electrons as they leave the metal for the solution may be considered as the cathodic current, i_c. The magnitude of the current flow, which is a measure of the velocity of these

[1] Manuscript received May 12, 1949. This paper prepared for delivery before the Chicago Meeting, October 12 to 15, 1949.

ionic and electron transitions, will be governed by any electrical potential difference existing at the metal-solution interface.

The functional dependence of the electron current, when electrons make transitions from the metal to the solution, on the electrode potential, $f_c(i_c)$, is usually designated as the cathodic polarization function and yields the well-known cathodic polarization curve, while that of the ionic current, when metal ions make transitions from the metal to the solution, $f_a(i_a)$, is designated the anodic polarization function. These polarization functions, as defined here, are in terms of the current density per square centimeter of apparent area of the electrode surface. They are, therefore, general functions and no assumptions are made as to the actual fraction of the apparent area that is cathodic or anodic. If the true cathodic and/or anodic areas are different from the apparent area and should vary during the polarization, the effect will be included in the polarizing functions $f_c(i_c)$ and $f_a(i_a)$. These functions also include all effects which may be present such as concentration polarization, overvoltage, ohmic resistance drops, etc.

When an electrode is placed in a solution containing an oxidation-reduction system and the electrode material takes part in the reaction so that the whole system is not in oxidation-reduction equilibrium, the measured electrode potential on open circuit may be called the "mixed potential" (11, 12). There will be a cathodic current i_c, whereby the oxidized system is being reduced and an anodic current i_a, whereby the metal ions are dissolving, and the two currents will be of equal magnitude on open circuit. This open circuit local action current may be designated i_0, and the open circuit electrode potential designated as E°.

If the electrode potential is varied by polarizing the electrode by an external means, the reaction velocities i_c and i_a will vary according to the polarization functions f_c and f_a. A possible set of polarization curves for some particular metal and oxidation-reduction system is shown schematically in Fig. 1*a*. Here, the curve a-b-c is the cathodic polarization curve, given by $f_c(i_c)$, for the reduction of the oxidized form of the oxidation-reduction system on the surface of this particular metal. We shall designate this as the "real" cathodic polarization curve for the oxidation-reduction system. The curve d-e is the anodic polarization curve, given by $f_a(i_a)$, for the metal. The point of intersection M represents the mixed potential E°, and the local action current i_0, in the steady state on open circuit.

It may be noted here that the reaction will be under diffusion control only if the curve d-e crosses the curve a-b-c at potentials more negative than point "b."

When the electrode is polarized by an external means, the electrode potential changes and the cathodic and the anodic currents will shift on their respective polarization curves, and for any given electrode potential there will be a corresponding value of i_a and i_c which may be read off the respective polarization curves d-e and a-b-c.

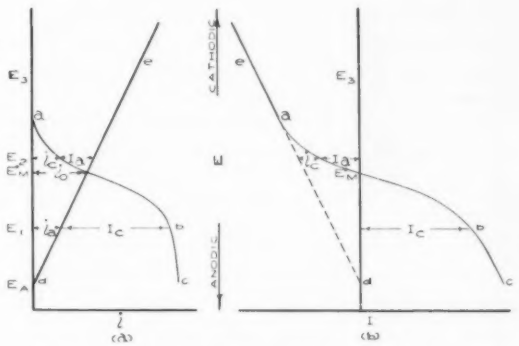

FIG. 1. (*a*) Schematic *self*-polarization curves for a metal and an oxidation-reduction system; (*b*) schematic *external* polarization curve when the metal is polarized by external means.

Thus, if the electrode is cathodically polarized to the potential E_1 by the application of an external cathodic current density I_c, the total cathodic reaction will be

$$i_c = i_a + I_c$$

as shown in the figure. On the other hand, if the electrode is anodically polarized to the potential E_2 by the application of an external anodic current density I_a, the total cathodic current will be

$$i_c = i_a - I_a$$

If the above electrode were polarized from the potential E_3 to E_4 by external means and the curve depicting E vs. I plotted, it would appear as curve e-a-b-c in Fig. 1*b*. We will designate this curve as the external polarization curve. Here I_c and I_a are the externally applied cathodic and anodic current densities, respectively. The extrapolated curve a-d is the portion of the anodic polarization

curve M-d of Fig. 1*a*. The "real" or actual cathodic current density on the electrode will be given as shown above by $i_c = i_a \pm I$, the plus or minus sign being used depending upon whether the external current I is cathodic or anodic.

Although the idea of a mixed potential, as presented here, may lead to the same results as the theory of local elements, we believe that the former presents a more generalized point of view. The mixed potential theory leads to the conclusion that there exists on a metal surface, which is undergoing dissolution, two or more independent electrochemical reactions which are only related by the electrical potential difference which exists between the metal and the solution. This notion of two independent electrochemical reactions on the same surface was also arrived at by Wagner and Traud (13). The theory does not depend upon the concept of local elements, although this latter concept comes under the theory as a special case.

Experimental

Materials and Apparatus

Pure aluminum (99.99) in the form of chill cast rods, 1.2 cm in diameter, and rolled sheet, 0.25 mm thick, was used. All solutions were made up with redistilled water and reagent grade chemicals. The compositions are given in Table I.

TABLE I. *Composition of the cerium sulfate solutions*

Solution	$Ce(SO_4)_2$	$Ce_2(SO_4)_3$	H_2SO_4
	moles/l	*moles/l*	*moles/l*
1	0.10	0.10	2.5
2	0.25	0.10	2.5
3	0.40	0.10	2.5
4	0.6	0.1	2.5
5	0.15	0.05	2.5
6	0.05	0.0	2.5
7	0.05	0.0	0.5
8	0.10	0.0	5.0

The electrode potential measurements were made with a potentiometer used in conjunction with a vacuum tube amplifier. A saturated calomel cell was used as the reference electrode and a glass tube, filled with the particular solution being studied, served as a salt bridge. One end of this tube was drawn down to a fine capillary and pressed close to the back of the electrode (14).

The electrolysis cell was a conventional H type cell which consisted of two separate compartments connected by a small bore tube. One of these compartments contained the electrode under study and the capillary tipped tube which made connection with the calomel cell on the outside. The volume of solution in this compartment was 300 ml. The other compartment contained a large platinum sheet, which served as the auxiliary electrode, immersed in 100 ml of solution. Two copper coulometers were placed in series with the cell during weight loss measurements.

Most of the experiments were run in a thermostatically controlled water bath where the temperature was controlled to ± 0.1°C. Although no appreciable difference was observed between results obtained in air free solutions and air saturated solutions, nitrogen was used in most of the experiments.

All the data presented were obtained with stationary electrodes and still solutions. All values of electrode potentials are given with reference to the saturated calomel electrode.

Procedure

The surface of the metal specimens was prepared as follows: The rods were turned on a lathe, polished with a coarse emery paper, and cleaned in nitric acid. They were then given a regular metallographic polish using a kerosene-paraffin mixture with the papers and finally obtaining a high polish with pure alumina. The sheet aluminum was polished with #0000 paper only and then cleaned in hot acetone, distilled water, and rubbed lightly with soft tissue and distilled water. Great care was taken in order not to leave any abrasive particles imbedded in the surface. The specimens were then weighed and all but a defined area of 2.0 to 10.0 cm^2 was coated with an insulating lacquer.

The data reported were obtained by the following three well-known types of measurements:

1. Time-potential and weight loss measurements were made on specimens exposed to the solutions on open circuit. The time varied from 30 minutes to about 5 hours.

2. External polarization curves were obtained as follows: The aluminum electrode was placed in the cell and allowed to stand on open circuit until a fairly steady potential was obtained; generally ten minutes sufficed. It was then polarized by the application of an external current. After the polarizations on any one aluminum specimen were completed, a platinum electrode of the exact shape

and size as the aluminum electrode was placed in the cell in exactly the same position and polarized. The purpose of the platinum experiment and the precautions taken was to obtain the limiting diffusion currents of the oxidation-reduction system on an inert electrode for any given solution and compare it with that obtained on aluminum.

3. The weight loss of the specimen was obtained after it had been exposed to the solution at a predetermined and constant potential. This was achieved by polarizing the aluminum electrode as above but regulating the externally applied current so that aluminum assumed and maintained a given potential for 3.0 to 5.0 hours. The average value of the external current was obtained from the coulometers. Although there was some drift in the required external current, the variations were generally less than 5 per cent and never greater than 10 per cent of the mean value.

In order to be sure that no appreciable ohmic voltage drop was being introduced due to the position of the capillary tip, experiments were performed with the tip placed at close contact and 3 mm away from the electrode. No appreciable differences were noted in the results.

The reactivity of the aluminum as indicated by its weight loss is given in all cases in terms of current per square centimeter of apparent area and designated as i_a. The externally applied current is expressed in a similar manner and designated I_a or I_c for external anodic and cathodic polarization, respectively.

Results

Time-Potential Behavior and Reactivity of Aluminum

The variation of the electrode potential with time was recorded and the weight loss was determined for many specimens on open circuit. On immediate immersion, the potential was very cathodic and then changed rather rapidly to more anodic values becoming fairly steady after about 10 minutes. The general behavior is shown in Fig. 2. The steady state potential on open circuit at 25.0°C was about 0.0 volt, ±0.1 volt in all of the solutions of cerium sulfate in sulfuric acid, while in sulfuric acid it was about −0.9 volt. While any given specimen maintained a steady state potential within a few centivolts, a variation of as much as a tenth of a volt was shown at times by different specimens.

The rate of dissolution of aluminum on open circuit at 25.0°C corresponds to about 0.4 ma/cm² in all of the cerium sulfate solutions when H_2SO_4 is 2.5M and is independent of the ceric sulfate concentrations and time of immersion used. It increases to about 0.5 ma/cm² when the H_2SO_4 concentration is increased to 5.0M and decreases to about 0.2 ma/cm² when the acid concentration is decreased to 0.5M. At 50.0°C the dissolution rate increases to about 2 ma/cm² in the cerium sulfate solutions when H_2SO_4 is 2.5M.

The variations of the dissolution rate from one specimen to another in any one solution were within 0.1 ma/cm².

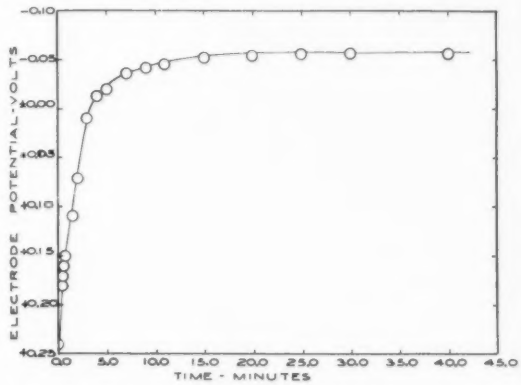

FIG. 2. Time-potential relationship in cerium sulfate solution 3 at 25.0°C.

Within these limits the results are more or less independent of the surface preparation. Thus, the specimens may be used immediately after preparation, or days afterward they may be etched with HCl to reveal grain structure before immersion or just cleaned in the as-cast or rolled state and yield about the same results.

No evolution of gas could be detected on the surface while on open circuit in the cerium sulfate solutions.

External Cathodic Polarization

Fairly well-defined external cathodic polarization curves were obtained on aluminum in all of the solutions. The curve consists of two waves, the cerium^{+4} reduction wave and the hydrogen ion reduction wave. A typical cerium^{+4} reduction curve is shown in Fig. 3 where the results were obtained on a specimen which was immersed in the solution for 24 hours. It was polarized soon after immersion and just prior to its removal. The limiting diffusion current for the cerium^{+4} sulfate reduction obtained

on aluminum was, in all cases, approximately the same as that obtained on platinum for any given solution.

The curves were quite reproducible and do not change appreciably with time of immersion. The curves on different specimens are almost identical except for some displacement of the whole curve on the E axis of about 0.1 volt; this displacement is due to the difference in open circuit potential of some specimens.

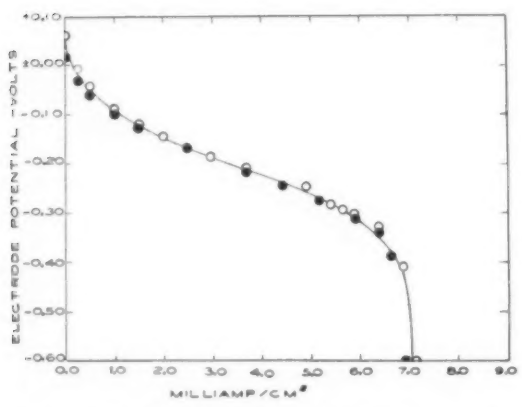

FIG. 3. External cathodic polarization curve for aluminum in cerium sulfate solution 4 at 25.0°C. The values plotted are I_c vs. E. ○—soon after immersion; ●—after 23 hours immersion.

TABLE II. *The limiting current density on aluminum and platinum, the electrode potential, and the reactivity of aluminum as a function of the cerium^{+4} sulfate concentration in 2.5M H_2SO_4*

$Ce(SO_4)_2$	$(I_c)_d$ on Pt	$(I_c)_d$ on Al	i_a on Al	E^0 Al
moles/l	*ma/cm²*	*ma/cm²*	*ma/cm²*	*volts*
0.05	0.8	0.8	0.4	−0.1
0.15	1.8	1.8	0.3	−0.1
0.25	3.8	3.7	0.4	±0.0
0.40	5.6	5.0	0.4	±0.0
0.6	6.5	7.0	0.3	+0.1

Generally, the open circuit potential, assumed by the aluminum immediately after a cathodic polarization had been performed, was more cathodic than the steady state value, and slowly recovered to the original value.

The data presented in Table II show how the limiting diffusion current for cerium^{+4} sulfate reduction on aluminum and on platinum, the rate of dissolution of aluminum, and the open circuit potential of aluminum depend upon the concentration of cerium^{+4} sulfate in solutions which were 2.5M with respect to H_2SO_4. It may be noted that the cerium^{+3}-cerium^{+4} electrode potential on platinum was in all cases about +1.2 volts and varied in a reversible manner with changes in the salt concentrations.

External Anodic Polarization

Many aluminum specimens were anodically polarized in 0.5, 2.5, and 5.0M sulfuric acid and in the various cerium sulfate solutions. Although the anodic polarization curve in H_2SO_4 is not linear when considered over a wide potential range, it is very close to a linear relation from the open circuit potential, −0.9 volt to about +1.5 volts. Since we are primarily concerned with this potential range in the present study, we may consider the curve as approximately linear. The slope of the curve is about 3000 ohms in 0.5M acid, and about 2000 ohms in 2.5 and 5.0M acid at 25.0°C. In the latter solutions it decreases to about 300 ohms at 50.0°C.

The anodic curves in the cerium sulfate solutions show a "wave," the upper part of which is linear. This linear section is almost identical to the anodic curve which is obtained in H_2SO_4 in the same potential region. When any one aluminum specimen was anodically polarized both in H_2SO_4 and in a cerium sulfate solution which had the same concentration of H_2SO_4, it was found that the linear section of the curve obtained in cerium sulfate lies a little above the curve obtained in H_2SO_4, but otherwise is almost identical to it. If the linear section of the curve obtained in cerium sulfate is extrapolated back to the potential axis, it is almost identical to the anodic polarization curve obtained in H_2SO_4. It was found that the value of the current on this extrapolated curve, which corresponds to the open circuit potential of the aluminum, is equal to the rate of dissolution of aluminum on open circuit, $i_3 = i_a$, in the particular solution as obtained by weight loss within about ±0.1 ma/cm².

A typical set of anodic polarization curves is shown in Fig. 4, where curve A was obtained in 2.5M H_2SO_4 and curve B in a solution of cerium sulfate in 2.5M H_2SO_4. At no time was there any evidence of a wave for the oxidation of cerium^{+3} sulfate.

These results strongly indicate that the extrapolated curve, obtained from the external anodic polarization in cerium sulfate, is the "self"

anodic polarization curve of aluminum.[2] In addition it appears that this self-anodic polarization curve is approximately the same as the anodic polarization curve for the aluminum in H_2SO_4 of the same strength, obtained by external polarization. It should, therefore, be possible to interpret the results by the use of the mixed potential theory.

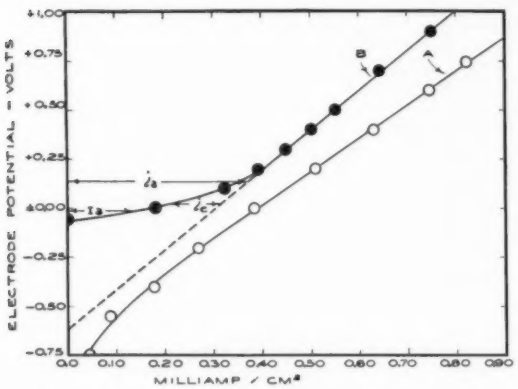

FIG. 4. External anodic polarization of aluminum (I_a vs. E). Curve A was obtained in 2.5M H_2SO_4 and curve B in cerium sulfate in 2.5M H_2SO_4.

Analysis of Polarization Curves

An analysis of the polarization curves was made in order to obtain the values of i_c, the "real" or total current density for the reduction of cerium^{+4} sulfate, and then the function $f_c(i_c)$. In order to do this, the curves were interpreted in the following manner. For any given solution of cerium sulfate in H_2SO_4, the linear section of the external anodic polarization curve was extrapolated back to the potential axis. From this extrapolated curve, the total anodic current density, i_a, and the total cathodic current density, i_c, which prevail from the open circuit potential E^0 through the range of more cathodic potentials, were obtained. The externally applied anodic current density is given by I_a and the following relation holds true: $i_a = i_c + I_a$. These current components are designated in the Fig. 4.

The values of I_c, the externally applied cathodic current density, were added to the values of i_a, as obtained above, in order to obtain the total cathodic current density i_c, which prevailed for any given potential E more anodic than the open circuit potential E^0. For this potential region we have $i_c = i_a + I_c$.

The values of i_c were then plotted versus the electrode potential in order to obtain the "real" polarization curve for the cathodic reduction of cerium^{+4} sulfate on aluminum. Typical curves obtained by the above procedure are shown in Fig. 5, 6, and 7. In each case, the self-anodic polarization curve of the aluminum is also shown. The curves in Fig. 5 and 6 show the effect of temperature, while that in Fig. 7 shows the effect of varying both the cerium^{+4} sulfate concentration and the temperature. The latter shows the interesting case where the entire cathodic polarization curve for the reduction of cerium^{+4} sulfate on the aluminum is obtained by an external anodic polarization of the aluminum.

Weight Loss Measurements

In order to confirm the above interpretation of the polarization curves, a series of aluminum specimens were polarized in 2.5M H_2SO_4, and another series in cerium sulfate solution 2. Two or more specimens of each series were polarized at a predetermined constant potential for 3 hours and the externally applied current density and the weight loss determined. In each series, various potentials ranging from +1.5 volts to −1.0 volt were chosen.

In addition, several experiments were performed in each of which a single specimen was polarized at several predetermined constant potentials, covering the same range as above, for 3 hours at each potential. The current density and weight loss were determined at each potential.

The results were interpreted as follows: for any given electrode potential the external current density gives I_c or I_a, depending upon whether the specimen was cathodically or anodically polarized; the weight loss corresponds to i_a and the total cathodic current density, i_c, is given by $i_c = i_a \pm I$, where the plus sign is for external cathodic polarization and the negative sign for the external anodic polarization.

From the values of i_c so obtained, the "real" cathodic polarization curve for the reduction of cerium^{+4} sulfate was constructed. A representative curve obtained by the second method is shown by the open circles in Fig. 5. It will be seen that the

[2] Polarization due to the local action currents as opposed to externally applied currents is designated "self" polarization. See GATTY AND SPOONER, "The Electrode Potential Behavior of Corroding Metals in Aqueous Solution," p. 25, Oxford University Press (1938).

general form of the curve confirms the results obtained by the regular polarizing technique.

The Cathodic Polarization Function

An analysis of many "real" cathodic polarization curves for the reduction of cerium^{+4} sulfate

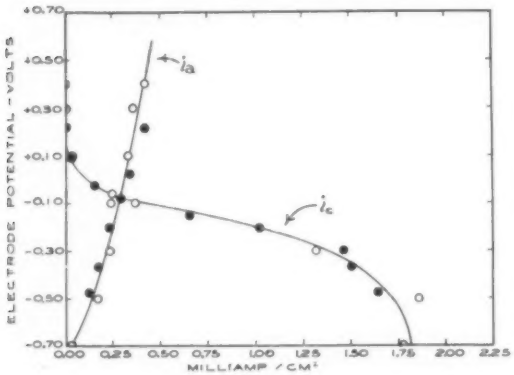

FIG. 5. The "real" polarization curve for the reduction of cerium^{+4} on aluminum and the self-anodic polarization of aluminum in solution 2 at 25.0°C. ○—the values of "i_c" and "i_a" were obtained from weight loss measurements as explained in the text; ●—the values were obtained from regular external polarization curves.

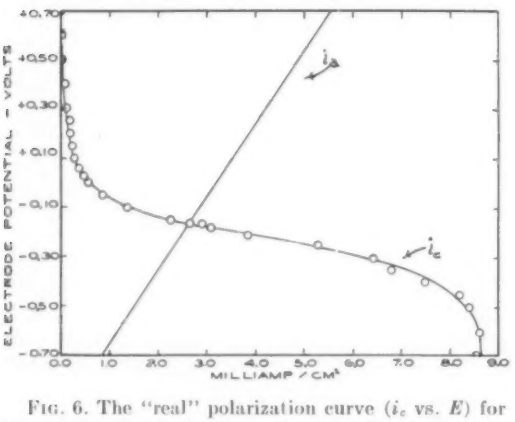

FIG. 6. The "real" polarization curve (i_c vs. E) for the reduction of cerium^{+4} on aluminum in solution 2 at 50.0°C.

on aluminum showed that the following relation approximates the curve fairly well:

$$E = b \log [(i_c)_d - i_c]/i_c - E_{\frac{1}{2}}$$

where E is the electrode potential, $(i_c)_d$ is the limiting current density, i_c the current density, b is a constant, and $E_{\frac{1}{2}}$ is a constant equal to the value of the potential when $i_c = (i_c)_d/2$.

The equation is compatible with the fact that no evidence of the oxidation of cerium^{+3} sulfate on the aluminum could be obtained. The values of E versus the log $[(i_c)_d - i_c]/i_c$ were plotted for all the data. A typical curve is shown in Fig. 8,

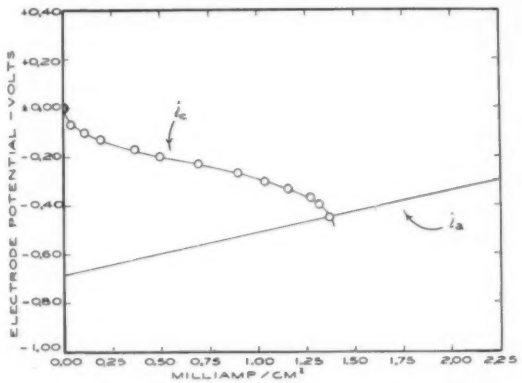

FIG. 7. The "real" polarization curve (i_c vs. E) for the reduction of cerium^{+4} on aluminum in solution 6 at 50.0°C.

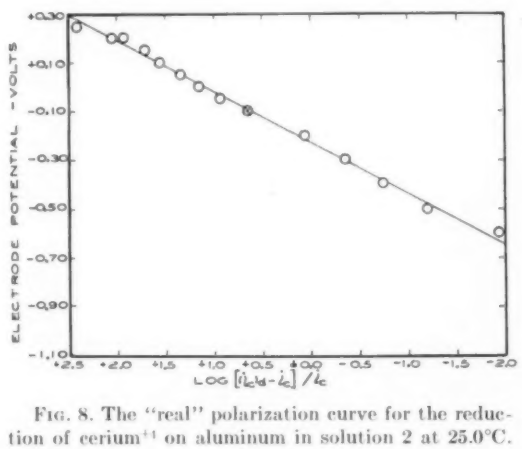

FIG. 8. The "real" polarization curve for the reduction of cerium^{+4} on aluminum in solution 2 at 25.0°C. X—designates open circuit values.

where the point designated as X is the open circuit value. Generally, although the slope of these curves, b in the equation, was constant for any one polarization, it did vary at times from one polarization to another. The extreme variations were from 0.12 to 0.30 while most of the values found were between 0.15 and 0.20. Some of these values as well as $E_{\frac{1}{2}}$ are given in Table III.

The results obtained in solution 7 which is only 0.5M in H_2SO_4 were generally similar to those ob-

tained in the stronger acid solutions except for a few cases. In some experiments, the aluminum became very passive during anodic polarization. When the anodic current density reached the neighborhood of 0.4 ma/cm², the potential became very positive (>+1.5 v) and the current density was decreased to a few ma/cm². If the external circuit was broken, the open circuit potential was about −0.4 volt. If the electrode was cathodically polarized while in this state, the usual cerium^{+4} wave was not obtained; the potential rose to that for hydrogen evolution and a hydrogen curve was obtained.

TABLE III. *The effect of solution composition and temperature on "b" and "$E_{\frac{1}{4}}$"*

Solution	Temp	b	$E_{\frac{1}{4}}$
	°C		
1	25.0	0.30	−0.15 v
2	25.0	0.18	−0.25 v
2	50.0	0.16	−0.23 v
3	25.0	0.18	−0.24 v
4	25.0	0.15	−0.20 v
6	50.0	0.14	−0.24 v
7	25.0	0.16	−0.30 v
8	25.0	0.23	−0.15 v

The electrode would recover to normal behavior if it was immersed in 12.0*N* HCl for a few seconds.

Surface Appearance

The following observations were made on the appearance of the aluminum surface after exposure to the various solutions. Exposure in any of the solutions at 25.0°C at the open circuit potential or more anodic potentials produced a mildly etched surface. On highly polished specimens, interference tints were observed in the more concentrated solutions of cerium sulfate on open circuit, while at 50.0°C interference tints were observed in all cerium solutions. Whenever the aluminum was anodically polarized, thus, exposed in the solutions at more cathodic potentials than the open circuit one, interference tints could be observed if the electrode was removed from the solution soon after the polarization. The interference tints became more pronounced the more cathodic the potential, and the lower the acid strength. The tendency for interference tints to form and the order of tinting seemed to be independent of the presence of cerium salts but strongly dependent on acid strength, temperature, and potential. The tints would disappear if the electrode stood on open circuit in the more dilute cerium sulfate solution or sulfuric acid, or was cathodically polarized after their formation.

In some cases, it was noted that a thin, loosely adhering white film formed at the edges, that is, very close to the lacquered edges. This readily wiped off, revealing the same tinted surface underneath as on the rest of the surface.

Discussion

Generally, the rate of dissolution, the electrode potential, and the polarization characteristics of pure aluminum in solutions of cerium sulfate and sulfuric acid are reproducible within relatively narrow limits. The results reported here are only a representation of a great many experiments. In some cases, the electrodes were studied over the course of days and it was found that the open circuit potential for any given specimen was constant to within a few centivolts and that repeated polarization curves from E^0 through the region of more anodic potentials were approximately superposable. There is a tendency, however, for the anodic branch of the curve to decrease in slope. Even when this change in the anodic branch takes place, the calculated "real" reduction curve or the cathodic polarization function remains about the same.

The above is particularly true in the more concentrated cerium sulfate solutions where $i_0 \ll (i_c)_d$; when this latter condition holds, it is not necessary to construct the "real" curve in order to obtain the cathodic polarization curve for the reduction of cerium^{+4} sulfate since, in this case, $i_c \cong I_c$. The curve shown in Fig. 3 is one of this type.

We have not, as yet, been able to explain why the linear section of the anodic curve in cerium sulfate solutions has a tendency to lie above the the curve obtained in sulfuric acid.

Unlike the cathodic curves, the slope of the anodic polarization curve is dependent on the particular specimen, surface preparation, and time of exposure in the solutions. Any one specimen, however, will give an approximately identical curve in sulfuric acid as the linear section of the curve in cerium sulfate.

The experimental results indicate in a qualitative manner, if not quantitatively, that the reaction of pure aluminum with cerium^{+4} sulfate may be interpreted by the theory of the "mixed poten-

tial." Thus, we are dealing with two separate reactions, the cathodic and the anodic, which are both governed by the electrode potential.

The thermodynamically reversible electrode potential of aluminum in acid solutions is about −1.9 volts (15) and, experimentally, has been found to lie close to this value for an amalgamated electrode (16). Mears and Brown (17) have found a difference of 3.0 volts in the electrode potential of aluminum with an oxide coating and with the film removed by continuous abrasion. In our own work, it was found that abrading the surface caused the potential to rise to more anodic values.

The anodic reaction in sulfuric acid and cerium sulfate, therefore, shows a large polarization effect. The polarization decreases with an increase in acid strength and an increase in temperature. It is, also, practically independent of the cerium sulfate concentration. Since there was no indication of the oxidation of cerium^{+3} sulfate, the anodic reaction is the dissolution of aluminum. These facts strongly indicate the formation of a film on the surface at all current densities and potentials studied. The formation of interference tints at various potentials and their variation with acid strength and temperature give visual evidence of the formation of a thin, compact and firmly adhering film on the aluminum surface.

The oxidation-reduction potential of cerium sulfate is about +1.2 volts on inert electrodes and, although the reduction of this system proceeds reversibly on platinized platinum, there is an overvoltage on white platinum (9). As the experimental results show there is a large overvoltage for the reduction of cerium^{+4} sulfate on aluminum.

It may be noted here that the cathodic polarization curve for cerium^{+4} on white platinum followed a course similar to that given by equation I for aluminum. The constant E_1, however, was close to +1.2 volts, but the values of b were very close to those obtained on the aluminum.

Equation I may be derived from the following expression when the theory of a diffusion current is taken into consideration (18).

$$i_c = k[\mathrm{Ce}(\mathrm{SO}_4^{=})_4^{=}]\bar{e}^{2.3E/b}$$

Accordingly, the concentration or, more rigorously, the activity $\mathrm{Ce}(\mathrm{SO}_4^{=})_4^{=}$ at the electrode surface for any given cathodic current density i_c is given by

$$[\mathrm{Ce}(\mathrm{SO}_4^{=})_4^{=}]\,\frac{1}{FD}\,[(i_c)\,d - i_c]$$

where "1" is the thickness of the diffusion layer, F is the Faraday, D is the diffusion coefficient for the ion, and $(i_c)_d$ is the limiting current density.

From this development it will be seen that

$$E_1 = b \log \frac{k1}{FD} + C$$

where the constant C will include the reference electrode potential and liquid junction potential, both of which are assumed constant in this work.

The data show a trend for E_1 to shift to more cathodic values with increase in acid strength and to be independent of temperature in the range of 25.0°C to 50.0°C. The latter may be due to the fact that any increase in the reaction rate constant k is offset by an opposite change in the ratio of $1/D$.

An examination of the two polarization functions for this system shows that the reactivity of the aluminum is under both anodic and cathodic control.

An attempt was made to explain the form of the polarization functions by assuming the presence of a porous oxide film on the surface of the metal, where the surface of the film acts as a cathode and the bare metal at the base of the pores the anodes. The argument followed very closely to Muller's theory (6), but no satisfactory progress was made.

As previously stated, the data reported here are only a part of a general study on the electrochemical behavior of aluminum and any detailed explanation of the mechanism involved will only be possible at the completion of the study. It may be desirable, however, to give an outline of an hypothesis which is being formulated as a result of this study. We, therefore, suggest the following tentative explanation for the electrode behavior of pure aluminum.

The aluminum is covered with a thin, compact, and continuous film of an amorphous oxide. In the solutions used here, the thickness of this film lies between a few ångströms to about 40 ångströms, depending upon the values of E, i_a, acid strength, and temperature. Aluminum ions can migrate and/or diffuse through the lattice of the oxide while the electrons can only pass through by means of the well-known quantum mechanical tunnel effect. An important feature of this concept is that there are no bare portions of the metallic aluminum surface in intimate contact with the solution. An electrical potential difference exists be-

tween the metal and the solution which maintains an electric field across the oxide film. This field reduces the height of the energy barrier for the outward flow of aluminum ions from the metal into the solution. At the same time, the potential difference and the film thickness govern the probability of electron penetration through the film.

In the steady state on open circuit, the potential difference and the film thickness will assume the values necessary for $i_a = i_c = i_0$. When the electrode is anodically polarized, the film becomes thicker and the potential more positive inwardly so that the probability of electron penetration decreases, while when cathodically polarized, the reverse changes in potential and film thickness take place and the probability of electron penetration increases. The changes in ionic migration, i_a, are in each case opposite to those for electron penetration.

A more detailed and quantitative development of these ideas is planned for the future.

Any discussion of this paper will appear in a Discussion Section, to be published in the December, 1950 issue of the JOURNAL.

REFERENCES

1. A. L. FERGUSON AND H. BANDES, *Trans. Electrochem. Soc.*, **81,** 273 (1942); A. L. FERGUSON, "Electrode Processes," Discussions of the Faraday Soc. No. 1, Gurney and Jackson, London (1947).
2. N. K. ADAM, "The Physics and Chemistry of Surfaces," p. 321, Oxford U. Press, London (1941).
3. WILLIAM H. COLNER, *Corrosion*, **3,** 11, Nov.–Dec. (1947).
4. T. P. HOAR, *Trans. Electrochem. Soc.*, **76,** 157 (1939).
5. For bibliography on electrochemical theory of corrosion see RALPH LANDAU, *Trans. Electrochem. Soc.*, **81,** 559 (1942).
6. WOLF JOHANNES MULLER, *Trans. Electrochem. Soc.*, **76,** 167 (1939).
7. U. R. EVANS, "Metallic Corrosion, Passivity and Protection," p. XXXIII, Longmans, Green and Company, New York (1946).
8. G. FREDRICH SMITH AND G. A. GETZ, *Ind. Eng. Chem. Anal. Ed.*, **30,** 191 (1938).
9. To be published.
10. F. SEITZ, "The Modern Theory of Solids," McGraw-Hill Publishing Co., Inc., New York (1943).
11. I. M. KOLTHOFF AND C. S. MILLER, *J. Am. Chem. Soc.*, **62,** 2171 (1940).
12. J. A. V. BUTLER, W. E. HUGH, AND D. H. HEY, *Trans. Faraday Soc.*, **22,** 24 (1926).
13. C. WAGNER AND W. TRAUD, *Z. Elektrochem.*, **44,** 391 (1938).
14. J. V. PETROCELLI AND ARTHUR PHILLIPS, *Trans. Electrochem. Soc.*, **85,** 257 (1944).
15. W. M. LATIMER, "Oxidation Potentials," Prentice-Hall, Inc., New York (1935).
16. LOUIS KAHLENBERG AND S. J. FRENCH, *Trans. Electrochem. Soc.*, **52,** 360 (1927).
17. R. B. MEARS AND R. H. BROWN, *Ind. Eng. Chem.*, **33,** 1006 (1941).
18. J. N. AGAR AND F. P. BOWDEN, *Proc. Roy. Soc. London*, **169A,** 206 (1938).

Polarographic Investigation of Mercaptobenzothiazole[1]

G. Sartori and A. Liberti

Istituto Chimico dell' Università di Roma, Italy

ABSTRACT

The cathodic and anodic behavior of mercaptobenzothiazole at the dropping mercury electrode has been investigated. It has been found that the anodic electrode reaction does not correspond to an oxidation to the disulfide, but to the formation of the mercurous compound Hg (mercap.). Only one electron is involved in the process and the diffusion coefficient has been found to be 6.3×10^{-6} cm²/sec.

An equation has been derived to interpret the experimental results: from the dependence of the half-wave potential on the pH, it has been possible to calculate the dissociation constant of mercaptobenzothiazole. This value is in agreement with the one obtained potentiometrically.

The catalytic nature of the cathodic waves has been demonstrated. The height of this wave, i.e., the current due to the catalytic evolution of hydrogen, is proportional to the hydrogen ion concentration of the buffer, and it depends on the concentration of the catalyst through a relationship given by the Langmuir isotherm.

Mercaptobenzothiazole is a chemical which is commercially important as a vulcanizing agent. Recent studies showed a promising use of this compound as an analytical reagent and as an intermediate product in the preparation of biologically active compounds.

In order to evaluate the possibilities of mercaptobenzothiazole in amperometric titrations, an investigation of this compound at the dropping mercury electrode has been carried out.

The sulfydryl-containing systems have been studied polarographically by Kolthoff and Barnum in connection with an investigation on cysteine, and by R. Brdička in relation to the catalytic waves. No complete investigations on the current voltage curves of mercaptan derivatives at the dropping mercury electrode have been reported in the literature.

G. Proske (1), in a study on vulcanization accelerators, reported that mercaptobenzothiazole might be determined by means of the polarograph. He describes reduction waves, which we have not been able to obtain, and attributes the reduction of mercaptobenzothiazole and related compounds to the presence of a double bonded nitrogen.

Experimental

Materials Used

Technical mercaptobenzothiazole [hereafter abbreviated H (mercap.)] was dissolved in sodium hydroxide and precipitated with hydrochloric acid. This treatment was repeated many times. The purified product was crystallized from acetic acid and recrystallized from ethanol (mp 176–178°C).

The purity of the product was checked by titration with silver nitrate following the Volhard method as described by Ushakow and Galanow (2), and amperometrically by means of a rotating platinum electrode, according to the method of Kolthoff and Harris (3).

H (mercap.) solution (0.02M) in ethanol is stable for a long time. A stock solution ($2 \times 10^{-2}M$) in alcohol was used in the preparation of varying concentrations. Because this substance is almost insoluble in acid medium, aqueous alcoholic solutions were prepared for the measurements. The ethanol content was about 25 per cent in volume.

For buffer solutions, the universal buffers of Britton and Robinson, unless differently specified, were used in the pH range 1.6–10.0.

Apparatus and Circuits

Both the manual apparatus similar to that described by Kolthoff and Lingane (4) and an automatic Leybold polarograph were used in this work. The saturated calomel electrode (S.C.E.) was the reference electrode for all potentials reported in this paper. All experiments were carried out in a thermostat at 25° ± 0.1°. Under the experimental conditions, the capillary has a drop time of 3.4 seconds at zero applied emf. The product $m^{\frac{2}{3}}t^{\frac{1}{6}}$ was 1.965. The current-voltage curves shown in the figures have been plotted without making any

[1] Manuscript received May 19, 1949. This paper prepared for delivery before the Chicago Meeting, October 12 to 15, 1949.

correction for the residual current, but all values of the current given in the tables and used in analyzing the waves have been properly corrected for the residual current.

Results

Anodic reaction of H (mercap.) at the dropping mercury electrode.—Mercaptobenzothiazole yields an anodic wave in buffered and unbuffered solutions in the pH range 1 to 13. In acid solutions of a pH lower than 5, another anodic wave is observed at a more positive potential. This wave is very irregular and has a maximum which is not suppressed by any suppressing agent. This wave does not yield reproducible diffusion currents.

Some of the experimental data are summarized in Table I.

TABLE I. *Wave heights and half-wave potentials in* $5 \times 10^{-4}M$ *solution of H (mercap.) at varying pH at* $25° \pm 0.1°$.

pH	π	Wave height
	volts	*μamp*
1.15	+0.066	1.45
2.86	−0.015	1.45
3.86	−0.075	1.45
4.44	−0.100	1.45
4.94	−0.125	1.50
5.57	−0.165	1.50
6.39	−0.205	1.45
6.88	−0.231	1.55
7.38	−0.255	1.50
7.65	−0.255	1.45
9.38	−0.255	1.45
10.0	−0.255	1.50
13.0	−0.255	1.45

A plot of the half-wave potentials from Table I against pH yields a straight line with a slope of 0.055 volts per pH unit up to pH 7, and is constant at higher pH values (Fig. 1). Table I shows that the diffusion current is fairly constant at varying pH values. It is a linear function of the concentration up to $5.0–7.5 \times 10^{-4}M$ H (mercap.) solutions. For higher concentrations, the wave levels off to give a constant current which depends on the pH and the nature of the buffer solution. Current voltage curves obtained at varying concentrations of H (mercap.) are presented in Fig. 2.

The formation of a film of mercurous mercaptide around the drop which prevents further interaction between mercury and H (mercap.) probably is responsible for this effect.

Fig. 3 shows the dependence of this limiting current on the pH of the buffer solution.

In order to have information on the nature of the anodic process, the number of electrons involved in the electrode reaction may be calculated by means of the Ilkovič equation. Since the diffusion coefficient of H (mercap.) is not known, we have assumed, as a first approximation, that H (mercap.) diffuses at the same rate as benzoic acid, and its diffusion coefficient is used in the calcula-

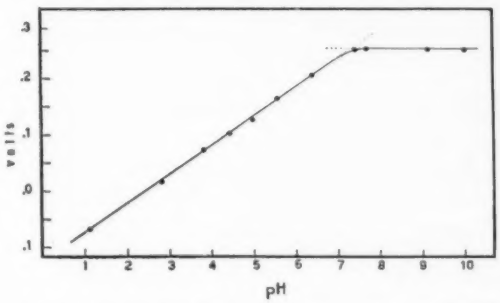

Fig. 1. Change of the half-wave potential vs. pH of the supporting electrolyte.

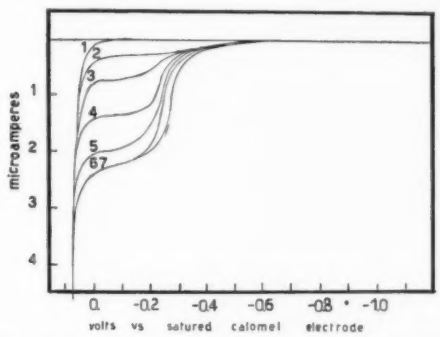

Fig. 2. Anodic waves of H (mercap.) in borate buffer (pH = 10) at various concentrations. (1) supporting electrolyte; (2) $10^{-4}M$; (3) $2.5 \times 10^{-4}M$; (4) $4.75 \times 10^{-4}M$; (5) $7.5 \times 10^{-4}M$; (6) $10^{-3}M$; (7) $1.5 \times 10^{-3}M$.

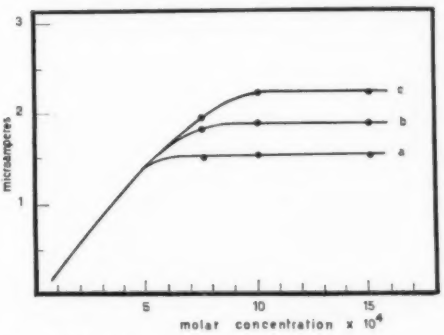

Fig. 3. Limiting current as a function of concentration at (a) pH = 1; (b) pH = 6.0; (c) pH = 10.

tion. The anodic reaction of H (mercap.) involves one electron per molecule ($n = 1$). From the Ilkovič equation $I_d = 605\ nm^{\frac{2}{3}}t^{\frac{1}{6}}DC$ the diffusion coefficient of H (mercap.) was calculated and found to be 6.3×10^{-6} cm²/sec in 0.1*M* acetate buffer at pH 4.9.

Discussion

Barron, Flexner, and Michaelis (5) reported that the mercury electrode is not an indifferent electrode to systems containing -SH groups. The anodic waves of cysteine obtained by Kolthoff and Barnum (6) do not correspond to a reversible oxidation to cystine but to the formation of a mercury compound. The analogy of this system with that of the cysteine permits us to formulate identical hypotheses; but since it has been calculated that only one electron is involved in the electrode reaction, we may, therefore, take into consideration only the formation of the mercurous compound.

This compound differs, however, from the mercurous cysteinate described by Kolthoff and Barnum because of its slight solubility. The film of Hg (mercap.) around the drop, which prevents a regular diffusion current, occurs in the entire range of pH and is only slightly affected either by acid or alkaline medium. Another proof of the slight solubility of the Hg (mercap.) is given by the following experiment: A solution $5 \times 10^{-4}M$ of H (mercap.) in 0.1*M* $HClO_4$ was electrolyzed in the absence of oxygen at a large quiet mercury electrode for twelve hours at a potential of +0.1 volt (potential corresponding to the diffusion current). After the electrolysis, a white precipitate was observed. The solution was filtered out and a stream of H_2S was bubbled through it; only a brownish turbidity was observed. This fact shows that only traces of soluble mercury were in the solution.

The reaction at the mercury drop leads, therefore, to the formation of mercurous mercap. and can be represented by the following expression:

$$\text{Hg} + \text{H (mercap.)} = \text{Hg (mercap.)} + \text{H}^+ + e \quad \text{(I)}$$

The reaction (I) can be expressed through the partial reactions

$$\text{Hg} = \text{Hg}^+ + e$$
$$\text{H (mercap.)} = \text{(mercap.)}^- + \text{H}^+$$
$$\text{Hg}^+ + \text{(mercap.)}^- = \text{Hg (mercap.)}$$

When a mercury electrode is in equilibrium with the surrounding liquid, its potential is given by the expression

$$\pi = \pi_0 + RT \ln \text{Hg}^+ \quad \text{(II)}$$

In the presence of H (mercap.) which depolarizes the dropping anode with the formation of a slightly soluble mercurous compound, reaction (II) becomes

$$\pi = \pi_0 + RT \ln \frac{L}{(\text{mercap.})^-}$$

where L is the solubility product of Hg (mercap.). The analytical concentration of mercaptobenzothiazole is given by the expression

$$C = \text{H (mercap.)} + \text{(mercap.)}^- \quad \text{(III)}$$

and taking into account K, ionization constant of H (mercap.)

$$(\text{mercap.})^- = \frac{CK}{K + [\text{H}^+]} \quad \text{(IV)}$$

By introducing (IV) in (III)

$$\pi = \pi_0 + \frac{RT}{F} \ln \frac{L}{CK}(K + [\text{H}^+]) \quad \text{(V)}$$

which may be written

$$\pi = \pi_0 + \frac{RT}{F} \ln \frac{L}{K} + \frac{RT}{F} \ln \frac{1}{C} + \frac{RT}{F} \ln (K + [\text{H}^+]) \quad \text{(VI)}$$

and combining all the constants in π_0' and introducing the diffusion conditions the following expression is obtained:

$$\pi = \pi_0' + \frac{RT}{F} \ln \frac{1}{(i_d - i)} + \frac{RT}{F} \ln (K + [\text{H}^+]) \quad \text{(VII)}$$

At the half-wave potential where $i = i_d/2$

$$\pi = \pi_0' + \frac{RT}{F} \ln \frac{1}{i_d/2} + \frac{RT}{F} \ln (K + [\text{H}^+]) \quad \text{(VIII)}$$

This equation points out that

$$\frac{\partial \pi_{\frac{1}{2}}}{\partial [\text{H}^+]} = \frac{RT}{F} \frac{1}{(K + [\text{H}^+]} \quad \text{and}$$

$$\frac{\partial \pi_{\frac{1}{2}}}{\partial \text{pH}} = -\frac{RT}{F} \frac{[\text{H}^+]}{(K + [\text{H}^+])} \ln 10$$

therefore, when

$$[\text{H}^+] \gg K \quad \frac{\partial \pi_{\frac{1}{2}}}{\partial \text{pH}} = -2.3 \frac{RT}{F} = -0.06$$

$$[\text{H}^+] \ll K \quad \frac{\partial \pi_{\frac{1}{2}}}{\partial \text{pH}} \cong 0$$

$$[\text{H}^+] = K \quad \frac{\partial \pi_{\frac{1}{2}}}{\partial \text{pH}} = -0.03$$

The plot of the half-wave potential against pH shows that the conditions of the above equations are fulfilled. From Fig. 1, the abscissa at the inflection point is calculated and pK = 7.2, i.e., the ionization constant of H (mercap.) K = 6.3×10^{-8} is obtained. To check this value, we have determined the ionization constant by potentiometric titration. For this purpose a 0.01*M* H (mercap.) solution in 50 per cent ethanol was titrated with 0.021*N* NaOH using a glass electrode and an electronic galvanometer. A pK = 7.5, i.e., an ionization constant K = 3.1×10^{-8} was measured. Owing to the different ethanol content of the two solutions, this value is in fairly good agreement with the one determined by means of the polarograph.

TABLE II. *Wave height of* $5 \times 10^{-4}M$ *solution of H (mercap.) at varying pH in 25 per cent ethanol at 25°.*

pH	Limiting current in μamp
2.4	79.5
2.62	26.4
2.85	16.3
3.1	10.2
3.65	7.2
4.08	4.8
4.5	3.4
5.06	1.7
6.0	1.4
7.0	1.1

The analysis of the wave fits in with equation (VII). A plot of log $(i_d - i)$ versus potential for solutions $4.75 \times 10^{-4}M$ in H (mercap.) at varying pH gave a straight line with the following slopes: at pH = 10, 0.066 volt; at pH = 6.0, −0.075 volt; at pH = 4.6, 0.070 volt.

From equation (VIII) it is seen that the half-wave potential is not constant, but varies with i_d. At H (mercap.), concentrations smaller than $7.5 \times 10^{-4}M$, we actually found the half-wave potential to change according to this expression. For example we found in a solution of pH = 10 at H (mercap.) = 2.5×10^{-4}, $\pi_{\frac{1}{2}} = -0.225$ (calcd. −0.216); at H (mercap.) = 5.0×10^{-4}, $\pi_{\frac{1}{2}} = -0.235$ (calcd. −0.234) at H (mercap.) = 7.5×10^{-4} $\pi_{\frac{1}{2}} = -0.245$ (calcd. = −0.244).

Cathodic Behavior

It has been observed that H (mercap.) in buffered solutions yields polarographic waves in the pH range 2.5 to 7. A maximum is present which is not suppressed by any addition agent. At pH lower than 2.5, the limiting current coincides with that due to the discharge of the hydrogen ion and no reliable measurements can be performed. At pH higher than 7, no wave is observed.

The experimental results are presented in Table II.

A plot of this limiting current against pH is given in Fig. 4. The height of the wave depends upon the concentration of the H (mercap.). The changes of the wave height with concentration of H (mercap.) at pH = 3.1 are reported in Table III. These figures are compared with the values calculated with the aid of a formula which will be described later.

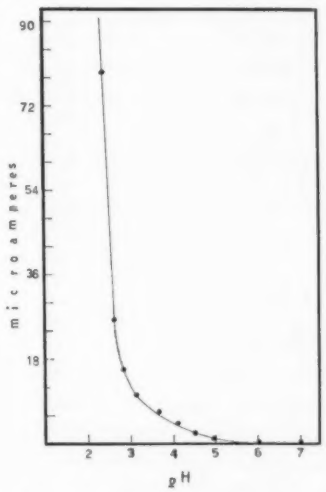

Fig. 4. Limiting cathodic currents of H (mercap.) ($2.5 \times 10^{-4}M$) at pH = 3.1.

Discussion

It has been pointed out by Brdička (7) that compounds, such as proteins, polypeptides, and amino acids containing the sulfhydryl group in certain buffer solutions, yield catalytic waves due to the lowering of hydrogen overvoltage.

It is evident also that the cathodic waves obtained in neutral and acid buffer solutions of H (mercap.) have to be regarded as due to a catalytic effect.

The height of this wave is much greater than would correspond to the number of electrons involved in any electroreduction process of H (mercap.). The H (mercap.) is, however, responsible for catalyzing the evolution of hydrogen.

By considering the Heyrovsky theory of hydro-

gen overvoltage, we may explain, according to Brdička, the mechanism of the catalyzed process with the following reactions:

$$\text{H (mercap.)} + e + \text{H} = \text{(mercap.)}^- + \text{H}_2$$
$$\text{(mercap.)}^- + \text{H}^+ = \text{H (mercap.)}$$

With this assumption the rate of reaction, i.e., the current intensity, is a function of the H (mercap.) concentration adsorbed on the cathode surface and of the proton concentration of the solution. This was found actually to be true: as far as the dependence on the pH is concerned, Fig. 4 shows a behavior very similar to the one found by Knobloch (8) for the catalytic wave of the amide of nicotinic acid. Since the catalytic waves of H (mercap.) are observed only in acid medium, we have to admit that the catalytic effect is due to the undissociated form of H (mercap.). However, we have been unable to find any relationship between the slope of the curve and the ionization constant of the proton donor.

The dependence of the catalyzed wave on the concentration of the catalyst follows the Langmuir adsorption isotherm in the Hückel formulation:

$$a = \frac{z\omega c}{1 + \omega c}$$

In this expression, a is the amount in moles of the substance adsorbed on the electrode surface, z is the maximum number of moles adsorbable on the electrode surface, ω is the adsorption coefficient, and c the analytical concentration of the adsorbable substance in moles per liter. According to our assumption, the adsorbable molecules are those of H (mercap.) and the height of the catalyzed wave, i.e., the current due to the catalytic evolution of hydrogen, is proportional to the amount of H (mercap.) adsorbed at the surface of the mercury. We substitute for a the observed values of the current in microamperes. We are able to calculate from any two different concentrations of H (mercap.) the two unknown constants of the above isotherm, viz. ω and z.

Thus we obtained $\omega = 544$ and $z = 46.8$. From these constants we have calculated the height of the catalyzed waves for any concentration of the H (mercap.) given in Table III. These calculated values are in fairly good agreement with the experimental values in the range of concentration investigated.

TABLE III

Concentration	i (measured)	i (calculated)
4.16×10^{-5}	1.56	1.05
9.95×10^{-5}	2.46	2.49
1.98×10^{-4}	4.71	4.59
3.92×10^{-4}	8.85	8.22
7.84×10^{-4}	15.0	14.1
1.78×10^{-3}	22.5	23.0

ACKNOWLEDGMENT

The authors acknowledge the help of Mr. Andrea Salvadore for his assistance in carrying out this work.

Any discussion of this paper will appear in a Discussion Section, to be published in the December 1950 issue of the JOURNAL.

REFERENCES

1. G. PROSKE, *Angew. Chem.*, **53,** 550 (1940).
2. M. I. USHAKOW AND A. S. GALANOW, *Z. anal. Chem.*, **99,** 185 (1934).
3. I. M. KOLTHOFF AND W. E. HARRIS, *Ind. Eng. Chem. Anal. Ed.*, **18,** 161 (1946).
4. J. J. LINGANE AND I. M. KOLTHOFF, *J. Am. Chem. Soc.*, **61,** 825 (1939).
5. E. S. G. BARRON, L. B. FLEXNER, AND L. MICHAELIS, *J. Biol. Chem.*, **81,** 743 (1929).
6. I. M. KOLTHOFF AND C. BARNUM, *J. Am. Chem. Soc.*, **63,** 3061 (1940).
7. R. BRDIČKA, *Collection Czechoslov. Chem. Communs.*, **5,** 148 (1933).
8. E. KNOBLOCH, *Collection Czechoslov. Chem. Communs.*, **12,** 407 (1947).

Effect of Thermal History on Color of Zinc Beryllium Silicate (Mn) Phosphors[1]

SHANNON JONES

Chemical Products Works, General Electric Company, Cleveland, Ohio

ABSTRACT

The fluorescent colors at room temperature of various completely-reacted manganese-activated zinc beryllium silicate phosphors can be changed by reheating them to temperatures lower than the original firing temperature with subsequent cooling at a rate in effect similar to the original cooling rate. A radical change in the cooling rate, as by quenching in water, also produces color shifts apart from the change due to reheating alone.

When a zinc beryllium silicate (Mn) phosphor is reheated at various temperatures from 700°C to 1200°C with subsequent normal cooling, shifts to the green occur in all cases with a maximum shift at 950°C. With increased time of refiring, especially at the higher temperatures, the colors shift back toward the original phosphor color.

With reheating and subsequent water quenching, the color shift to the green increases almost linearly with temperature over the range 800°C to 1200°C and extrapolates to zero color shift at 700°C. The magnitude of the color shift is greater with quenching than with normal cooling.

The data require two equilibrium approach rates for interpretation. The first or rapid change involves the equilibrium of manganese between its red-emitting and green-emitting states, with the green-emitting structure predominating at high temperatures. The second or slow change involves the migration of beryllium between substitutional positions either for silicon or zinc in the crystal. The equilibrium favors the beryllium-for-zinc substitution more for higher temperatures.

The beryllium position in turn modifies the manganese-state distribution, and this third equilibrium between the primary equilibria accounts for the time dependence of the color shifts.

INTRODUCTION

The relations of compositions and firing temperatures to the fluorescent colors of manganese-activated zinc beryllium silicate phosphors are well known to workers in this field (1, 2, 3, 4, 5). However, it has been found that the thermal history of this phosphor subsequent to the completion of the firing also has an effect on the fluorescent color obtained. The influence of the thermal history is shown by the color changes produced when the phosphor is reheated to various temperatures for various times. Following the reheating, the color shift depends in a complex manner on whether the phosphor is quenched in water or is allowed to cool in air.

EXPERIMENTAL PROCEDURE AND RESULTS

The color shifts produced by reheating were determined for four different types of zinc beryllium silicate (Mn) phosphors. The four phosphors are described qualitatively as yellow, yellow-pink, pink, and strong pink. Their approximate compositions are shown in Table I.

The color shifts produced by reheating and quenching in water have been determined only for the yellow-pink phosphor; the shifts produced by reheating and air-cooling are given for all four phosphors.

The data given in Tables II–VI show the percentage increase in the green-to-red intensity ratio under 2537 Å radiation.

For example, in Table II, for 5 minutes at 1210°C, the value 28.8 shows that the green-to-red ratio (G/R) of this phosphor was 128.8 when the G/R of the original phosphor was arbitrarily taken as 100. The green and red intensities were measured separately by using suitably filtered barrier-layer photocells and the ratios were computed from the measurements.

The reheating procedure was as follows: for each determination, about five grams of the

[1] Manuscript received April 21, 1949. This paper prepared for delivery before the Cleveland Meeting, April 19 to 22, 1950.

phosphor were put into a quartz boat, plunged into a furnace at a temperature and for a time indicated in the tables, then brought out quickly, and either quenched in water or allowed to cool in air on the boat.

Discussion

It is known that the various colors of zinc beryllium silicate phosphors are the result of the superposition of at least two distinct spectral bands which may change in relative intensity, breadth, and possibly position as the compositions and temperatures of the phosphors vary (1, 6).

Schulman has pointed out that beryllium may substitute for either silicon or zinc, or both, in

TABLE I. *Phosphor compositions in moles*

	Yellow	Yellow-pink	Pink	Strong pink
SiO_2	1.0	1.0	1.0	1.0
ZnO	1.59	1.71	1.59	1.54
BeO	0.08	0.29	0.32	0.34
MnO	0.080	0.105	0.145	0.145

zinc beryllium silicate, i.e., in the terminology of the chemist, beryllium oxide is amphoteric and behaves either as a basic or acidic group depending on the remainder of the composition (4).

In this discussion we shall take for granted this amphoteric nature of beryllium. We shall also assume that the green band is associated with manganese atoms substituting for zinc in the zinc silicate or zinc beryllium silicate lattice. On the other hand, in view of the diverse theories concerning the source of the red emission we shall make no assumptions as to the source of this band except that it is associated with manganese in a different environment from that responsible for the green band (4, 7, 9).

Now let us examine the data in Table II. We see that we obtain a greener phosphor when we quench from higher temperatures. If we plot the color changes in the 15 minute column against temperature, we find a fairly linear curve which extrapolates to zero change at about 700°C. It would seem to be justifiable to assume that by quenching we freeze in place manganese states which are predominantly green-emitting.

In Table II we also note that the influence of time is greater at higher temperatures. In view of the short times used, it might be thought that this is evidence of failure of the material to reach a temperature equilibrium. However, considerations of the effectiveness of radiative heat transfer at the various temperatures suggest that the effect is real.

From the color shift with time at high temperature refiring followed by quenching, it appears

TABLE II. *Per cent increase in G/R on reheating and water-quenching the yellow-pink phosphor*

Temp	5 min	15 min
°C		
1210		35.0
1100	28.8	31.5
1000	24.5	25.2
900	18.0	18.1
800		9.6

TABLE III. *Per cent increase in G/R on reheating and air-cooling the yellow-pink phosphor*

Temp	Time in minutes						
	5	15	30	45	135	405	960
°C							
1200	4.9	4.8		2.6			
1100	8.8	8.2		7.6	6.3		
1000	11.5	11.2			9.8		
900	10.8	10.8		10.0	10.8		
800		7.3		6.9			
750			4.0			5.1	
700							4.7

TABLE IV. *Per cent increase in G/R on reheating and air-cooling the yellow phosphor*

Temp	Time in minutes		
	15	45	135
°C			
1100			8.0
1000	14.4		10.3
900	13.9	11.2	
800	9.4	8.4	

plausible not only that the red-emitting state is unstable at high temperatures, but that at any temperature, an equilibrium between the red-emitting and green-emitting states exists. Most of the temperature-induced change of state requires a time of at least a few seconds, otherwise we could not freeze the state by water quenching. Furthermore, some change of state continues to take place for from five to fifteen minutes at higher temperatures.

Now when we examine the data in Tables III, IV, V, and VI, we find that the effects of refiring

followed by air cooling are qualitatively different from the effects produced by quenching. We note in Table III that a maximum in the shift to the green occurs at about 950°C. Furthermore, the green shift, especially at the higher temperatures, decreases with time.

This phosphor in its original preparation had cooled rather slowly from 1250°C to room temperature as a result of the large mass of material. We would estimate that the phosphor had spent at least five minutes in the 950° to 1050°C range. Thus it is surprising to find that reheating at 1000°C (or 900° or 1100°C) with subsequent air-cooling results in a considerably greener phosphor. The first thought is that as a result of the small amount of material refired, we have a slight quenching effect. However, the results on reheating at 1210°C, which with subsequent water quenching gives a greener phosphor, show that this is not the case. In fact, extrapolation of the data of Table III to 1250°C shows that reheating to 1250°C with this faster air-cooling does not appreciably change the color; in other words, our experimental air-cooling does not affect the phosphor much differently from the normal cooling of rather large batches.

TABLE V. *Per cent increase in G/R on reheating and air-cooling the pink phosphor*

Temp	Time in minutes		
	15	45	135
°C			
1100			5.4
1000	8.6		6.2
900	8.5	7.7	
800	7.5	5.2	

In the case of water-quenching, we would estimate that the phosphor cools to room temperature in a few seconds, while with air-cooling, the phosphor reaches room temperature in a few minutes. Thus we would say that the cooling rates are in a ratio of about 100 to 1. The quenching effects show that the assumed red-green state equilibrium is not essentially complete in a second or so, otherwise we could not freeze the green state so readily. On the other hand, the reversal of the shift to the green with air-cooling and increasing refiring times shows that a second rearrangement, much slower than the first manganese-state equilibrium rate, must be introduced to account for the data. It is also apparent that this slow rearrangement opposes the effects of the faster manganese-state equilibrium.

Let us assume that the slow rearrangement is a migration of beryllium atoms between zinc-substitutional and silicon-substitutional positions. Furthermore, let us assume that the beryllium-for-zinc substitution is favored at higher temperatures, and that this substitution forces manganese out of its green-emitting state (zinc substitutional position) into a position where it is in a red-emitting state. By this scheme, we can account for the decrease in G/R with increased time at a given temperature followed by air cooling.

TABLE VI. *Per cent increase in G/R on reheating and air-cooling the strong pink phosphor*

Temp	Time in minutes		
	15	45	135
°C			
1100			26.4
1000	26.9		27.9
900	28.7	27.0	
800	27.4	28.4	

Now if we assume that air-cooling rate is such that the fast equilibrium can follow the temperature change on air-cooling but that the slow (beryllium migration) equilibrium lags, then the shift to the red on cooling is increased by the failure of the beryllium to migrate rapidly from the zinc-substitutional (red-producing) to the silicon-substitutional position. Since these equilibrium rates are dependent on temperature, we can account for the maximum shift to the green at 950°C by assuming suitable values for the various rates at various temperatures. This hypothesis can account for the influence of temperature, time at a given temperature, and the subsequent cooling rate on the fluorescent colors obtained.

These equilibrium rates should also depend on the composition of the phosphor. This is indicated in Table VI, where the strong pink phosphor, which had a high manganese content, showed a large color shift on reheating, but little temperature or time dependence.

X-ray diffraction patterns of the quenched yellow-pink phosphor showed a barely perceptible contraction of the lattice as compared with the original sample (8). This effect is anomalous in the sense that an increase of the beryllia content

in a formulation not saturated with beryllia produces a redder phosphor while causing a contraction of the lattice. Thus in spite of the fact that the color was greener due to the frozen high-temperature manganese state, the hypothesis that beryllia tends to substitute slowly for zinc at high temperatures is supported.

It seems plausible that some of the effects of higher temperature firings in increasing the redness of zinc beryllium silicate phosphors have been due to the cooling from a higher temperature, rather than exclusively to a more complete reaction.

It would be of interest to prepare zinc beryllium siliciate phosphors of identical color when fired similarly but having radically different compositions. This is possible since silica, beryllia, and manganese individually modify the fluorescent color of this phosphor, with an increase in the proportion of any one of the three increasing the redness within a range limited by the remainder of the composition. Studies of reheating effects on these phosphors should be elucidating.

Any discussion of this paper will appear in a Discussion Section, to be published in the December 1950 issue of the JOURNAL.

REFERENCES

1. G. R. FONDA AND F. SEITZ (editors), "Preparation and Characteristics of Solid Luminescent Materials," p. 258, paper by Studer and Gaus, John Wiley & Sons, Inc., New York (1948).
2. *Ibid.*, p. 69, paper by G. R. Fonda.
3. *Ibid.*, p. 269, paper by Luke Thorington.
4. *Ibid.*, p. 406, paper by J. H. Schulman.
5. W. E. FORSYTHE AND E. Q. ADAMS, "Fluorescent and other Gaseous Discharge Lamps," p. 117, Murray Hill Books, Inc., New York (1948).
6. K. H. BUTLER, *J.* (*and Trans.*) *Electrochem. Soc.*, **93,** 143 (1948).
7. F. A. KROEGER, "Some Aspects of the Luminescence of Solids," Elsevier Publishing Co., Inc., New York (1948).
8. G. R. FONDA, Private Communication.
9. E. NAGY, *J. Optical Soc. Am.*, **39,** 42 (1949).
10. S. H. LINWOOD AND W. A. WEYL, *J. Optical Soc. Am.*, **32,** 443 (1942).
11. N. J. KREIDL, *J. Optical Soc. Am.*, **35,** 249 (1945).

Ultraviolet Emitting Phosphor[1]

RUDOLPH NAGY, R. W. WOLLENTIN, AND C. K. LUI

Research Department, Westinghouse Electric Corporation, Bloomfield, New Jersey

ABSTRACT

A calcium zinc phosphate phosphor activated with thallium has been developed for the generation of ultraviolet radiation and is especially rich in erythemal region. The peak of emission of this phosphor is dependent upon the ratio of the calcium to zinc. A phosphor in which 8 per cent of calcium is replaced by zinc in calcium phosphate has a peak emission at 3120 Å, or very near that of maximum erythemal effectiveness.

Forty-watt fluorescent lamps made with this new phosphor in ultraviolet transmitting glass (9821) produced between 7.5 to 8.7 watts of ultraviolet radiations between 2800 Å and 3800 Å with a peak emission at 3120 Å. The weighted erythemal effective radiation from this lamp is from 1300 to 1750 milliwatts, or about two and one half times the effective erythemal radiation from calcium phosphate activated with thallium.

When it is considered that these lamps operate from an ordinary fluorescent ballast and are more efficient than any other source in producing erythemal radiations, a new avenue of approach is open for bringing the benefits of sunlight into schools, offices, and factories.

INTRODUCTION

In the past the use of ultraviolet radiations has been limited largely to direct application with high intensities to produce erythema, vitamin D, and tanning. This, however, is not the way man is exposed to ultraviolet in nature. During summer months or in the tropics, he is submitted continuously to a varying degree of the sun's short radiations. In the winter months very little, if any, ultraviolet radiations are received from the sun.

There are a large number of substances which emit erythemal ultraviolet radiations when excited by x-rays or very short ultraviolet radiation. Unfortunately, there are only a few phosphors that have the efficiency or stability to make them useful in practical lamps. Clapp and Ginther (1) and Froelich (2) have reviewed various ultraviolet emitting phosphors. Of these, the most promising phosphors for the generation of erythema-producing radiations are calcium silicate activated by lead or thallium and calcium phosphate activated by thallium alone. However, the efficiency of these phosphors is not very high for erythema evoking radiations. The peak of emission for calcium phosphate is at 3280 Å, whereas that of calcium silicate is at about 3350 Å. The effective erythema-producing radiations have their peak at 2967 Å (Fig. 1, curve 1).

This paper reports a new phosphor having its peak emission at 3115 Å and yielding more than twice the erythemal efficiency of calcium thallium phosphate phosphor. It will enable irradiation with ultraviolet energy, duplicating closely the conditions found in nature.

EXPERIMENTAL

After a number of preliminary experiments with different ultraviolet emitting phosphors, the most promising material for further experimentation appeared to be a calcium phosphate. About thirty-five different elements were substituted for a portion of the calcium cation. In this manner, several new phosphors were synthesized whose emission spectra were closer to the desired wavelength of 2967 Å. The most pronounced shift in the emission spectrum was obtained when zinc was used to replace a portion of the calcium in calcium phosphate activated with thallium.

The preparation of the ultraviolet emitting phosphor can best be accomplished by reacting the salts in the dry state. Tricalcium phosphate, 0.9 mole, zinc phosphate, 0.06 mole, and thallium phosphate, 0.022 mole, are ballmilled together and fired in silica trays in an electric furnace for 1 hour at 1000°C. The thallium activator is very volatile at this temperature and only a small fraction of the original amount added remains in

[1] Manuscript received May 23, 1949. This paper prepared for delivery before the Philadelphia Meeting, May 4 to 7, 1949.

the phosphor. Prolonged heating will slowly deactivate the phosphor by removing the thallium from the lattice. Since thallium is very toxic, it is necessary to use the same precautions as when dealing with other poisonous metallic vapors.

Spectral energy distributions were made with a Beckman spectrophotometer on small patches of the phosphor irradiated with a quartz Sterilamp.[2] Fig. 2 shows the spectral energy distribution of different calcium thallium phosphate phosphors when various amounts of zinc were substituted for calcium. The peak of emission is shifted toward the shorter wavelengths as the amount of zinc is increased. The shift is more pronounced at low percentages of zinc.

[2] Trade-mark Reg., U. S. Pat. Office.

X-ray diffraction studies indicated that a contraction of the calcium orthophosphate lattice resulted with increasing mole per cent of zinc, as would be expected from the relative sizes of the two ions.

Preliminary measurements of the erythemal output of the phosphor were made by the plaque method (Fig. 3). Small plaques of exactly the same size were exposed to radiations from a quartz Sterilamp. The emitted erythemal radiations were read by a zirconium phototube WL-767 using a 9700 filter and an amplifier. Measurements of the response of the zirconium cell showed that the long wavelength cut-off very nearly approximated the erythemal effectiveness curve in this region. In this manner, a large number of samples could

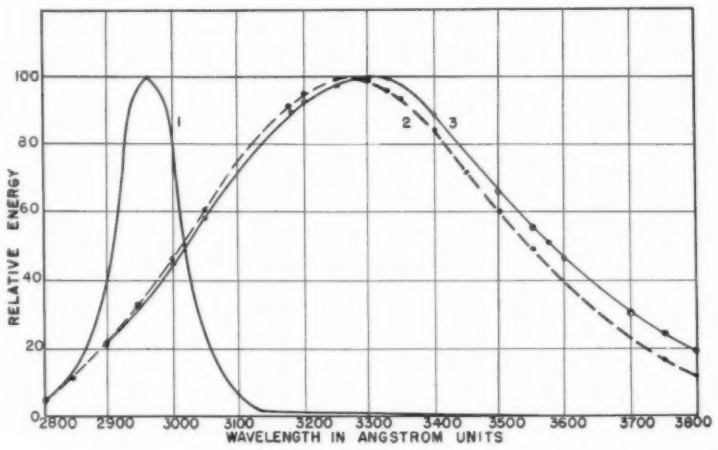

FIG. 1. (1) Spectral erythemal effectiveness, and the spectral energy distribution of (2) calcium thallium phosphate, (3) calcium lead silicate.

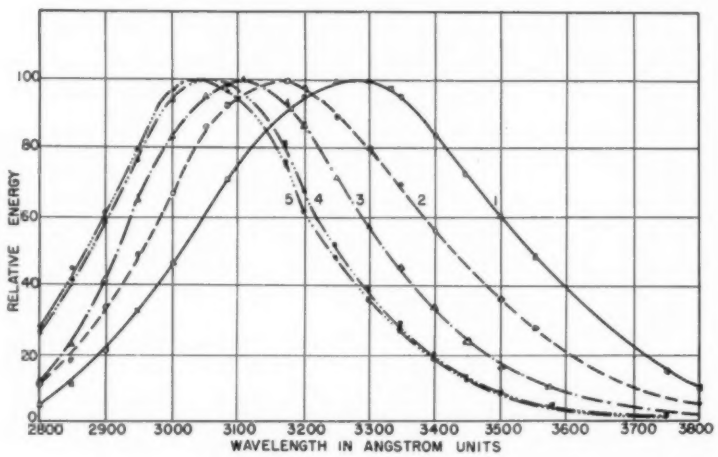

FIG. 2. Spectral energy distribution of calcium thallium phosphate substituted with various amounts of zinc phosphate (1) 0 mole %, (2) 4 mole %, (3) 8 mole %, (4) 10 mole %, (5) 12 mole %.

be rapidly compared for their relative erythemal output.

Measurements of the spectral energy distribution and of the total ultraviolet energy emitted from 40 watt fluorescent sunlamps were made for us by the National Bureau of Standards. The data were given in microwatts per square centimeter for 5 millimicron bands of wavelengths, at a distance of 3 meters from the center of the lamp. The phosphor was coated on 9821 glass in the normal manner and made into lamps. However, in order to obtain the maximum erythemal output, it was necessary to apply only a very thin coating. The spectral energy distribution of a lamp in 9821 glass is given in Fig. 4. The total emitted ultraviolet energy of such a fluorescent sunlamp varies from 7.5 to 8.7 watts depending upon the thickness of the glass and phosphor coating. The secondary peak at 3630 Å represents the mercury line 3650 Å.

To determine the amount of erythemal energy emitted from the lamp, the energy at various wavelengths was multipled by the erythemal effectiveness at the corresponding wavelengths proposed by the International Committee on Illumination (3). This gives a total of 1300 to 1750 milliwatts of effective erythemal energy from a 40 watt sunlamp. Skin tests, based on the value

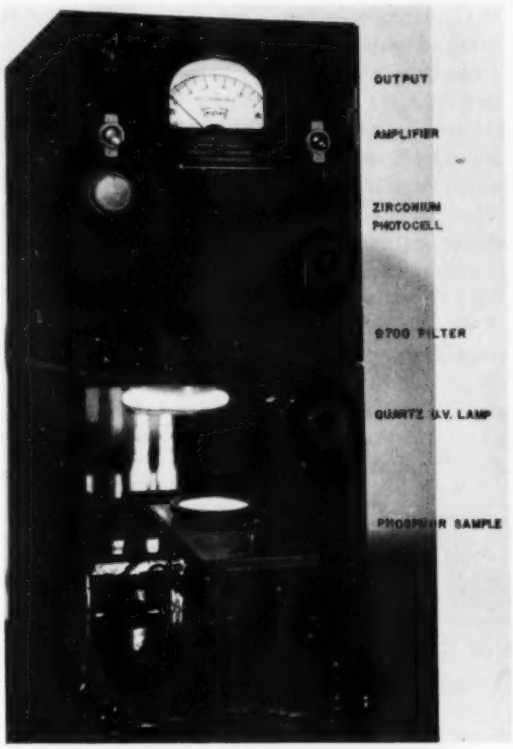

FIG. 3. Apparatus for measuring the erythemal response of phosphor powders.

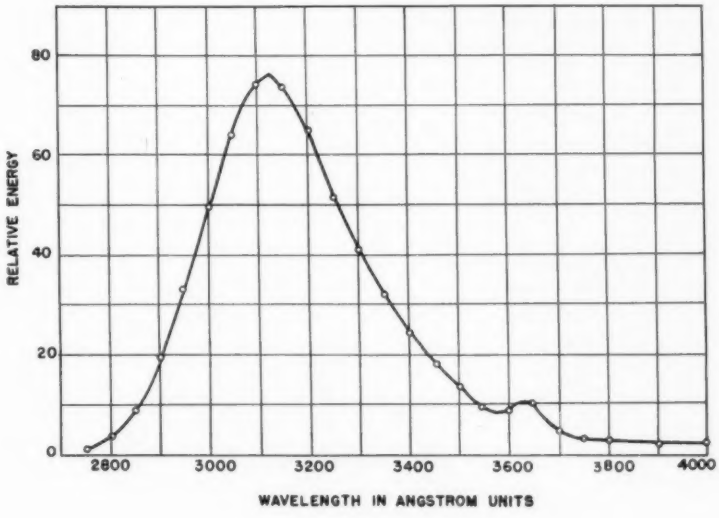

FIG. 4. Spectral energy distribution of a fluorescent sunlamp made with calcium zinc thallium phosphate phosphor in 9821 glass.

of 18 milliwatts-seconds per square centimeter on untanned skin as a minimal perceptible erythema, proved the above output to be very nearly correct. It must be remembered that there is considerable variation in the response of different individuals and that such tests are only indicative of the approximate magnitude of a lamp output.

Lamps made from Vycor glass indicate that the erythemal energy between 2500 Å and 3200 Å can be increased by at least 25 per cent. However, since it is necessary to apply a very thin coating of phosphor for maximum erythemal output, a considerable amount of 2537 Å radiations would also be emitted. It is for this reason that 9821 glass is used which unfortunately does not have a very sharp cut off and absorbs some of the erythemal radiations.

Discussion

The gradual shifting of the peak of emission of calcium thallium phosphate by the addition of increasing increments of zinc strongly suggests that this element modifies the crystal constants. X-ray diffraction studies show a contraction of the lattice, but retention of the calcium phosphate structure. The shifting of the fluorescence to shorter wavelengths has also been observed with additions of magnesium and potassium to calcium phosphate phosphor. The effect of potassium on the shift to the shorter wavelength has been reported by Clapp and Ginther. However, the erythemal energy from sunlamps made from these phosphors was much less than from calcium zinc thallium phosphate.

When compared on the basis of emitted erythemal energy fluorescent sunlamps made from calcium zinc thallium phosphate are much more efficient than any other source and more than twice as efficient as a sunlamp made with calcium thallium phosphate phosphor. This is so because the peak of emission has been shifted to lower wavelengths, and, therefore, a greater proportion of the energy falls within the erythemal band. Since the bactericidal and antirachitic action bands extend to 3200 Å, this phosphor will also be more than twice as efficient in destroying bacteria and producing vitamin D than the best calcium thallium phosphate. Thus there is now available an inexpensive source of space erythemal energy for therapeutic use, for prevention of rickets in both man and animals, for tanning or cosmetic applications, and for various photochemical processes.

Any discussion of this paper will appear in a Discussion Section, to be published in the December 1950 issue of the Journal.

References

1. R. H. Clapp and R. J. Ginther, *J. Optical Soc. Am.*, **37**, 355–362 (1947).
2. H. C. Froelich, *Trans. Electrochem. Soc.*, **91**, 241–261 (1947).
3. International Commission on Illumination, *Compte Rendu des Seances*, 1935, p. 596, Cambridge (1937).

Zinc Sulfide Infrared Quenching Phosphors[1, 2]

NATHAN T. MELAMED

Polytechnic Institute of Brooklyn, New York

ABSTRACT

The infrared quenching bands of zinc sulfide, activated by copper and by manganese, iron, nickel, or cobalt, were measured. They were found to be the same for each of the latter four activators. They are, therefore, attributed to the presence of copper. The quenching bands of copper activated zinc sulfide are similar to the stimulation bands of copper activated zinc sulfide containing either lead or manganese. Infrared stimulation and quenching are, therefore, believed to result from the same process. From measurements of photoconduction and the effect of cadmium sulfide on infrared quenching, the quenching bands are shown to be due to both deep and shallow traps associated with the auxiliary activator. A model is proposed for these traps.

Two types of infrared-sensitive phosphors of zinc sulfide are known: those whose emission is stimulated and those whose emission is partially or totally quenched by infrared irradiation. Both types apparently require the presence of two activators. In the infrared stimulable group is zinc sulfide activated either by copper and lead, or by copper and manganese. These phosphors have been described by Fonda (1). Urbach (2) has shown that the stimulation of the zinc sulfide, lead-copper phosphor is dependent upon the concentration of the copper ion. In the infrared quenching group is zinc sulfide activated with copper or with silver and with one of the elements iron, cobalt, or nickel. The latter have long been known as poisoning agents since, in excessive amounts, they cause a large decrease in the intensity of luminescence of either copper or silver activated zinc sulfide. In concentrations of the order of 10^{-6} moles per mole of base material they induce infrared quenching of either the copper or silver emission without unduly decreasing their phosphorescence.

EXPERIMENTAL PROCEDURES

Preparation of Samples

Samples were prepared by adding solutions of the activators to a weighed amount of zinc sulfide, together with a small amount of sodium chloride as a flux. For activation with lead, however, it was more convenient to add a weighed amount of solid lead sulfate. The mixtures were evaporated to dryness at 90°C and dried by heating at 200°C. They were then thoroughly ground in a drybox or dust-free hood, placed in small silica glass test tubes, and heated in a silica combustion tube at temperatures of 800° to 1200°C in an atmosphere of prepurified nitrogen. The heating period was from one half to one hour. Some of the samples were prepared as $\frac{3}{8}$ in. (0.95 cm) cylinders by molding the powder at a pressure of 35,000 pounds prior to heat treatment. Except for the lead phosphors the concentration of activators is given as moles of activator per mole of base material.

Description of Apparatus

The properties of the phosphors which were of especial interest in this work are emission spectra, quenching and stimulation spectra, and photoconductivity.

Quenching and stimulation bands were measured with the aid of the apparatus shown schematically in Fig. 1. It consisted of an 8 in. (20 cm) spherical mirror A with a $\frac{1}{2}$ in. (1.27 cm) hole at its center. The phosphor was mounted at B and a photocell was fixed at C, the conjugate focus of B. Corning filters No. 3389 and 5031 and a filter consisting of a 5 per cent solution of copper sulfate were mounted at D to shield the photocell from

[1] Manuscript received August 10, 1949. This paper prepared for delivery before the Philadelphia Meeting, May 4 to 7, 1949.

[2] The main part of this work was carried out under contract NObsr 39045 between the Polytechnic Institute of Brooklyn and the Bureau of Ships. This paper is abstracted from part of a thesis submitted by Nathan T. Melamed in partial fulfillment of the requirements for the degree of Doctor of Philosophy at the Polytechnic Institute of Brooklyn.

ultraviolet and infrared radiations. This assembly was enclosed in a box painted black on the inside. A Beckman quartz spectrophotometer was used as a source of monochromatic infrared of variable wavelength and intensity. The phosphor was excited by a beam of ultraviolet passing through a hole in the top of the box. Measurements of quenching or stimulation as a function of wavelength of infrared were obtained under equilibrium conditions with simultaneous infrared and ultraviolet irradiation. The intensity of irradiation was generally calculated on the basis of an equal number of photons at each wavelength of infrared, although the results so obtained did not differ significantly from those obtained on the basis of equal energy irradiation.

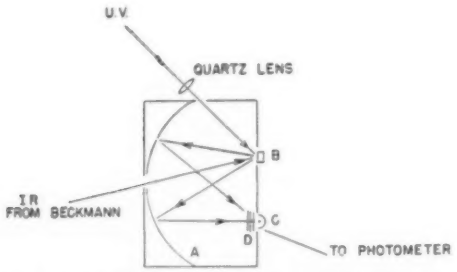

FIG. 1. Apparatus for measuring quenching and stimulation bands.

Emission spectra were obtained by means of a constant deviation spectrometer equipped with a Pellin-Broca prism. The phosphor was mounted near the entrance slit and was illuminated from above by an ultraviolet lamp. A source of infrared, placed in front of the phosphor, made it possible to compare the emission spectrum of the phosphor irradiated with infrared and ultraviolet with the spectrum obtained with ultraviolet alone. A 931 Å photomultiplier tube placed at the exit slit was used to measure the intensities of emitted light at different wavelengths. The measurements obtained were corrected for the spectral sensitivity of the phototube and the dispersion of the prism.

Measurements of photoconductivity were made with a sample 1 mm x 1 mm x ¼ mm which was mounted in an electrode assembly. Two opposite edges of the sample were painted with a conducting silver paint to obtain good electrical contact between electrode and sample. The photocurrent was measured by means of a direct coupled amplifier employing a 959 acorn tube as an electrometer tube. Three 45-volt dry cells in series supplied the d-c field. The Beckman spectrophotometer was used as the source of infrared. The entire assembly was shielded, and shielded coaxial cables of minimum length were used as leads. The photocurrents were too small to be corrected for polarization, hence the actual magnitudes of the photocurrents are in error. Polarization effects were kept to a minimum by keeping the time required for each measurement as short as possible and by depolarizing the sample between readings.

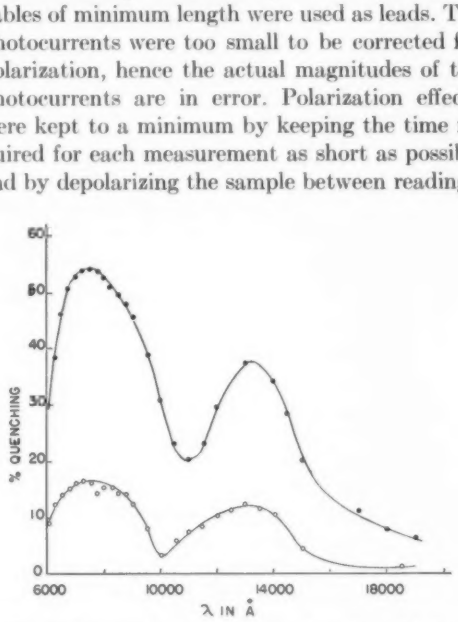

FIG. 2. Per cent quenching as a function of infrared wavelength. ●—ZnS:Cu 10^{-6} moles/gram, Co 10^{-8} moles/gram; ○—ZnS:Cu 10^{-6} moles/gram, Co 10^{-8} moles/gram.

EXPERIMENTAL RESULTS

Infrared Quenching Phosphors

Quenching bands.—Because cobalt is the most effective of the quenching activators, the zinc sulfide, copper-cobalt phosphor was studied first. A qualitative investigation of the wavelengths which produced quenching indicated that, with this phosphor, quenching can occur by irradiation with wavelengths as short as 4700 Å. At shorter wavelengths excitation takes place. In the region of 4700 Å, excitation and quenching probably occur simultaneously. Quantitative measurements using the apparatus of Fig. 1 indicated the presence of two quenching bands with maxima at 13,000 Å and 7800 Å. Fig. 2 shows the results obtained with two phosphors containing different amounts of cobalt. The apparatus, unfortunately, did not permit accurate measurements of quenching at wavelengths shorter than 6000 Å so that the short wavelength side of the 7800 Å band was not established.

In order to determine which of the activators

gave rise to the quenching bands, measurements were performed with zinc sulfide activated with copper and with manganese, iron, cobalt, or nickel. The results given in Fig. 3 show that the quenching bands for each of these activators are the same. Hence they are due either to copper or to the zinc sulfide. Attempts were made to measure quenching bands of zinc sulfide phosphors activated with silver in place of copper, but the results were inconclusive since the phosphors exhibited a greenish phosphorescence indicative of copper contamination.

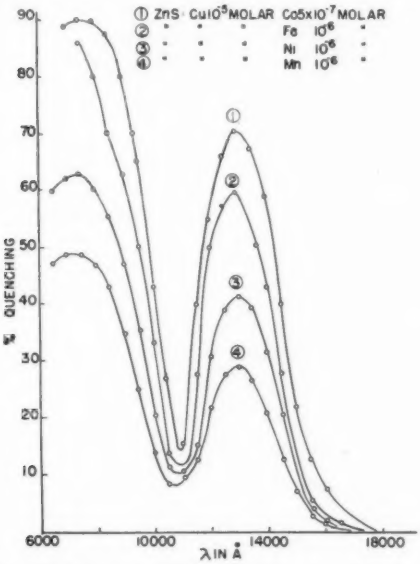

FIG. 3. Per cent quenching as a function of wavelength for different activators.

Photoconductivity.—Measurements of photoconductivity were made using a sample of composition ZnS: 10^{-4} Cu, 10^{-6} Co. The results for photoconductivity as a function of wavelength of irradiation are shown in Fig. 4. The sharp rise in photoconductivity at 5000 Å is due to excitation. Two other bands are present with maxima at 7800 Å and 12,000 Å. As has been previously mentioned, the results are not corrected for polarization, hence the bands are probably somewhat distorted. The results are sufficient, however, to show that photoconduction occurs when the phosphor is irradiated in the quenching bands.

The photoconduction due to the 7800 Å band was found to be dependent on the previous state of excitation. For a totally exhausted phosphor, no photoconduction occurred with 8000 Å irradiation. If the phosphor was excited for a period of time, then allowed to decay until no dark current could be detected, exposure to 8000 Å

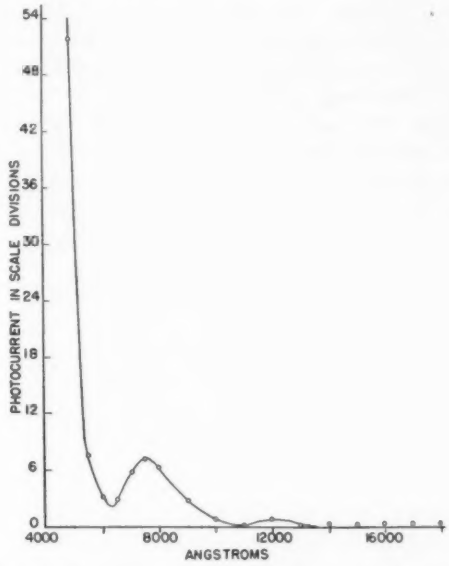

FIG. 4. Photocurrent as a function of wavelength of irradiating light.

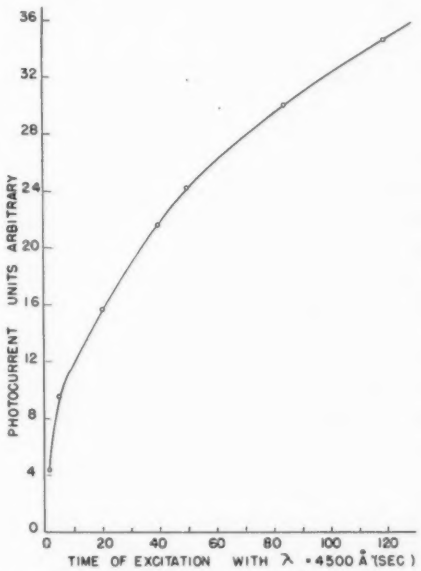

FIG. 5. Photocurrent due to 8000 Å irradiation as a function of time of 4500 Å excitation.

radiation resulted in photoconductivity. The dependence of photoconducitivity under 8000 Å illumination as a function of time of excitation

is shown in Fig. 5. The photoconductivity eventually reached a maximum value after long periods of excitation and remained constant after additional excitation. These results indicate that the 7800 Å band is a deep trap.

Effect of cadmium sulfide.—In order to determine whether the base material is responsible for the quenching bands, these bands were determined for samples of zinc sulfide containing various amounts of cadmium sulfide. It is well known that cadmium sulfide forms solid solutions

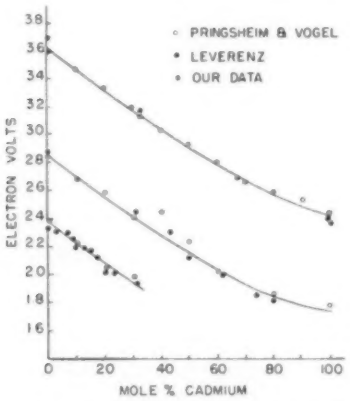

FIG. 6. Changes in absorption edge and emission peaks of ZnS activated by Ag or Cu due to addition of CdS.

with zinc sulfide and that the addition of cadmium sulfide to zinc sulfide activated with silver or copper causes the emission of these activators to shift toward longer wavelengths. In a similar manner, the absorption edge of the base material is also shifted to longer wavelengths. The emission peaks and the absorption edge of the base material as functions of cadmium sulfide concentration are given in Fig. 6 for two series of (Zn, Cd)S phosphors activated with silver and with copper. Some of the points are taken from published data (3, 4). The ordinate, plotted in electron volts, indicates that, as the concentration of cadmium sulfide increases, there is a uniform decrease in energy of emission and absorption. On the basis of the band model for luminescence, Randall (5) has suggested that this phenomenon may be the result of a lowering of the conduction band with respect to the ground state and activator levels due to the introduction of cadmium sulfide. The positions of the activator levels with respect to the ground state are assumed to remain substantially constant.

To check the effect of cadmium on the quenching bands, samples of composition ZnS, XCdS, 10^{-4} Ag, 10^{-6} Co, where X was 0.5 and 10 mole per cent, were used. The results of measurements using these phosphors are shown in Fig. 7 which gives the positions of the quenching bands. Although the addition of cadmium sulfide caused a shift of the emission and absorption edge toward longer wavelengths, it is clear that no shift occurred in the 13,000 Å quenching band. This

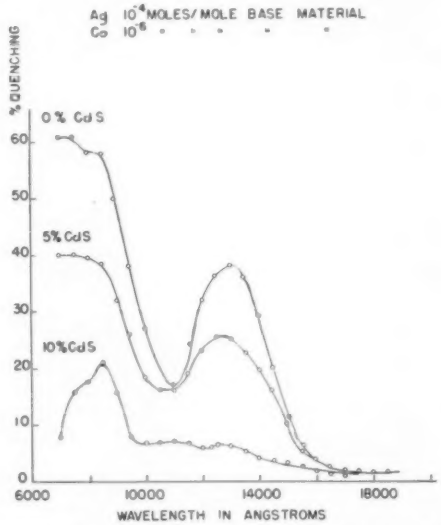

FIG. 7. Per cent quenching vs. irradiating wavelength for solid solutions of ZnCdS.

conforms to the results reported by Fonda (1) concerning the stimulation band of the zinc sulfide, lead-copper phosphor. It would, therefore, seem reasonable to suppose that the 13,000 Å band arises from an electronic transition between two levels lying below the conduction band and not from a transition directly to the conduction band. There appears to be a shift of the 7800 Å band to somewhat longer wavelengths, but uncertainty of the measurements does not permit such a close interpretation. An examination of Fig. 6 indicates that the addition of 10 per cent cadmium sulfide results in a decrease in energy of 0.1 electron volts. In the case of the 7800 Å band, this would result in a shift from 7800 Å to 8300 Å, a difference of only 500 Å, whereas a similar decrease in energy of the 13,000 Å band would result in its displacement to 14,500 Å, a difference of 1,500 Å. The location of the peaks of the quenching bands could not be obtained with

cadmium sulfide concentrations greater than 10 per cent.

It can be seen from Fig. 7 that the per cent quenching decreases with increasing concentration of cadmium sulfide. In order to measure the

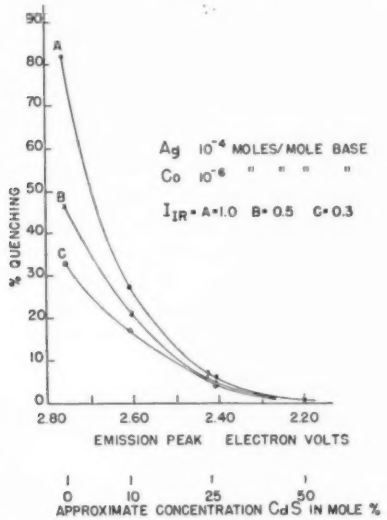

FIG. 8. Per cent quenching as a function of CdS content at 3 infrared intensities.

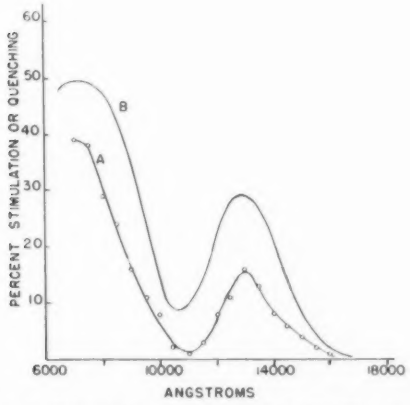

FIG. 9. Stimulation bands of ZnS:Cu:Pb phosphor compared with the quenching bands of a ZnS:Cu:Co phosphor. A—ZnS:Cu 10^{-4} moles/gram, 3 per cent $PbSO_4$; B—ZnS:Cu, Co for comparison.

per cent quenching as a function of greater cadmium sulfide concentrations than was possible with the apparatus used for measuring quenching bands, a more intense beam of infrared than could be obtained from the Beckman was necessary. The apparatus employed for measuring emission spectra was used, the per cent quenching being measured at the emission peak of the phosphor. (Previous measurements had shown that the per cent quenching is uniform over the measurable portion of the emission band.) The filter used for the infrared source had a transmission band with a maximum at 12,500 Å with no detectable transmission at wavelengths shorter than 9000 Å. Fig. 8 shows the per cent quenching obtained with three different intensities of infrared as a function of cadmium sulfide concentration. The abscissa is plotted in terms of both the approximate concentration of cadmium sulfide and the peak wavelength of the emission ex-

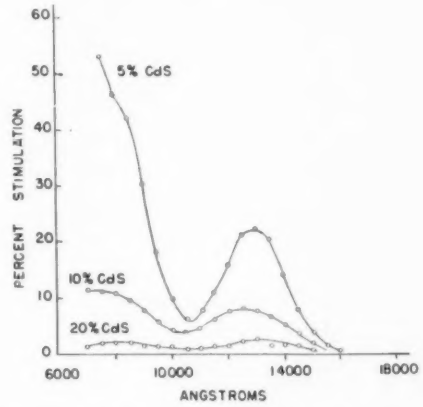

FIG. 10. Per cent stimulation vs. irradiating wavelength for solid solutions of ZnCdS activated by Cu and Pb.

pressed in electron volts. It is seen that increasing the amount of cadmium sulfide decreases the per cent quenching and that infrared quenching no longer occurs above 50 mole per cent of cadmium sulfide. Inasmuch as the phosphorescence decreases with addition of appreciable amounts of cadmium sulfide and is no longer present at concentrations greater than about 50 mole per cent, infrared quenching by the 13,000 Å band is presumed to be dependent on the presence of phosphorescence traps.

Infrared Stimulating Phosphors

Stimulation bands.—The two well-known infrared-stimulating phosphors of zinc sulfide are those activated with copper and lead, or with copper and manganese. Both are reported to have the same stimulation bands (1). The stimulation bands of the ZnS, Cu-Pb phosphor have been reported (2, 6). The stimulation bands of a ZnS,

Cu-Pb phosphor are shown in Fig. 9, together with the quenching bands of a ZnS, Cu-Co phosphor for comparison. The stimulation and quenching bands are identical.

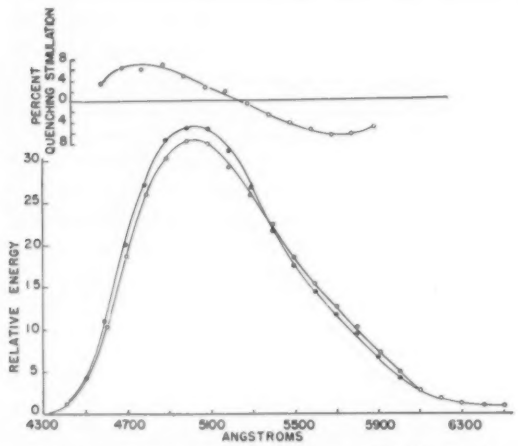

FIG. 11. Emission spectrum of ZnS, 5% CdS Cu 10^{-6}, 4% $PbSO_4$, under continuous excitation, with and without infrared irradiation. The per cent quenching and stimulation as a function of wavelength are shown above. ○—No infrared; ●—infrared on.

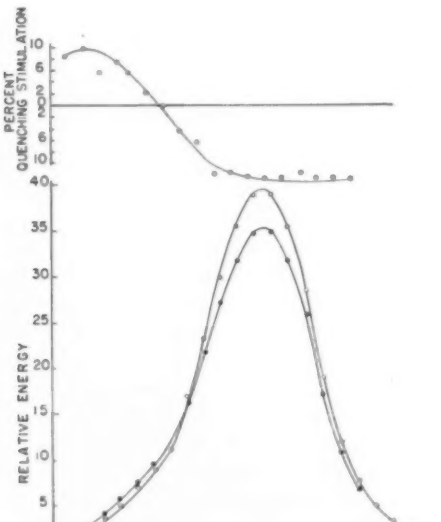

FIG. 12. Emission spectrum of ZnS, 10% CdS, Cu 10^{-4}, 3% $PbSO_4$ under continuous excitation, with and without infrared irradiation. The per cent quenching and stimulation are shown above. ○—No infrared; ●—infrared on.

Effect of cadmium sulfide.—Fig. 10 shows the stimulation bands for ZnS, Cu-Pb phosphor containing different amounts of cadmium sulfide. A comparison of Fig. 10 with Fig. 7 shows cadmium sulfide to have the same effect on the stimulation bands as it has on quenching bands. In ZnS, Cu-Pb phosphors, Urbach (2) regards copper as the auxiliary activator and attributes to it the stimulation bands. Since the quenching bands of the zinc sulfide-copper phosphors are also due to copper, it is reasonable to suppose that the role of copper is the same in both types of phosphors. Inasmuch as infrared irradiation causes the stimulation of the emission of the dominant activator, in this case lead, we might expect a simultaneous quenching of the copper emission

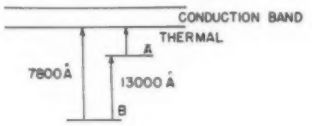

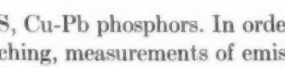

FIG. 13. A model for the traps which give rise to the 13,000 Å and the 7800 Å infrared sensitive bands.

in the ZnS, Cu-Pb phosphors. In order to observe this quenching, measurements of emission spectra were made.

Emission spectra.—Emission spectra for two (Zn, Cd)S, Cu-Pb phosphors are shown in Fig. 11 and 12. The emission spectra were measured under continuous ultraviolet excitation with and without infrared irradiation. The copper and lead emission bands for (Zn, Cd)S, Cu-Pb phosphors are sufficiently close together so as not to be readily distinguishable. The estimated positions of their peaks are indicated on the two figures. The phosphor whose emission spectrum is illustrated in Fig. 11 contained 10^{-6} moles of copper per mole of zinc sulfide. The dominant effect of infrared is to produce stimulation of the lead band. It is apparent, however, that simultaneous quenching of the copper band occurs under infrared irradiation. The per cent stimulation and quenching are plotted along the same wavelength scale at the top of the figure. The sample chosen for Fig. 12 contained a greater concentration of copper, 10^{-4} moles per mole of band, and the

dominant effect observed is the quenching of the copper emission by the infrared. The simultaneous stimulation of the lead emission is quite evident, however. A more extended study of the phenomenon in the zinc sulfide, manganese-copper phosphor has been made (7).

Discussion

The results obtained with the zinc sulfide, lead-copper phosphors appear to establish a fundamental connection between the processes of stimulation and quenching. Both phenomena are caused by absorption in the same bands, although the stimulation occurs in the emission of the dominant activator whereas quenching is confined to the auxiliary activator emission. Urbach (8) reported that the quenching bands for singly activated strontium sulfide-bismuth phosphors are identical with the stimulation bands of the strontium sulfide, bismuth-cerium phosphor. He regards this as a general property of all auxiliary activators. With regard to those zinc sulfide phosphors which contained iron, cobalt, or nickel in conjunction with copper, no stimulation has been observed, although in all other respects they behave in a manner similar to the zinc sulfide, copper-lead or zinc sulfide, copper-manganese phosphors. It is reasonable to suppose, therefore, that the transitions occurring within the activators iron, cobalt, or nickel are either nonradiative or have emissions in the near infrared. On the basis of absorption measurements made on zinc sulfide activated with these elements, we have concluded that they are similar to manganese and that a red or infrared emission is to be expected. A red emission has been attributed to iron (9, 10).

It appears fairly certain that the phosphorescence traps are involved in the stimulation and quenching processes, at least with regard to the 13,000 A band. This conclusion derives some support from the observations of Fonda and the behavior of the zinc sulfide, copper-lead phosphor at low temperatures (1). The nature of the 7800 Å band is not so clear, for reasons previously mentioned. The model presented in Fig. 13 attempts to relate the 7800 Å and 13,000 Å bands and is presumed to be equally valid for infrared stimulated phosphors as well as for quenching phosphors. Qualitatively it may explain some of the results obtained by other investigators on infrared phosphors, such as the slow buildup of phosphorescence during the initial stages of stimulation which has been reported by Ellickson for the strontium selenide, europium-samarium phosphor (11). Such an effect would be expected if the stimulation were affected by irradiation in the band which corresponds to the 13,000 Å band in zinc sulfide. Since the 13,000 Å transition is a two step process, of which the step of an electron going from level A to the conduction band is thermally activated, infrared stimulation should be temperature dependent and should decrease with decreasing temperature. Such effects have been observed by Garlick (12).

Acknowledgment

The author wishes to thank Professor Roland Ward for his guidance and encouragement.

Any discussion of this paper will appear in a Discussion Section, to be published in the December 1950 issue of the Journal.

REFERENCES

1. G. R. Fonda, *J. Optical Soc. Am.*, **36,** 374 (1946).
2. D. Pearlman, N. R. Nail, and F. Urbach, "Preparation and Characteristics of Solid Luminescent Materials," Chapter 21, John Wiley & Sons, Inc., New York (1948).
3. P. Pringsheim and M. Vogel, "Luminescence of Liquids and Solids," p. 84, Interscience Publishers, New York (1946).
4. H. W. Leverenz, Final Report, Contract NDCrc 150, June 30, 1945.
5. J. Randall, *Proc. Phys. Soc. London*, **49,** suppl. p. 46 (1947).
6. B. O'Brien, "Preparation and Characteristics of Solid Luminescent Materials," Chapter 7, John Wiley & Sons, Inc., New York (1948).
7. Michael Yamin, "The Effect of Activator Concentration on the Infrared Quenching and Stimulation of the Phosphor Zinc Sulfide, Copper-Manganese," B.S. Thesis, Polytechnic Institute of Brooklyn, 1949.
8. F. Urbach, D. Pearlman, and H. Hemmendinger, *J. Optical Soc. Am.*, **36,** 372 (1946).
9. A. Bundel, A. Rusanova, and E. Yakavlava, *Bull. acad. sci. U. R. S. S. Sèr phys.*, **9,** 542 (1945).
10. D. Pearlman, Private Communication.
11. R. T. Ellickson, *J. Optical Soc. Am.*, **39,** 64 (1949).
12. G. Garlick and D. Mason, *J.* (*and Trans.*) *Electrochem. Soc.*, **96,** 90 (1949).

Articles from Constitution Affecting Membership*

ARTICLE II

Membership:

Section 1. The membership shall consist of active members, student associate members, associate members, sustaining members, and honorary members.

Section 2. A candidate for active membership shall: be interested in the subject of electrochemistry or allied subjects; be at least 25 hears of age; and possess a Bachelor of Science or Engineering degree; and have three or more years of post-graduate experience in the phases of electrochemistry that are represented by the several Divisions of the Society. The post-graduate degree of Master of Science (or of Engineering) shall be equivalent to one year of experience, and the Doctor's degree in Science (or in Engineering) shall be equivalent to three years' experience. In lieu of a scholastic degree, ten years of experience shall be required in one or more phases of interest of the Society as represented by its several Divisions. Election to active membership shall require in addition recommendation by two active members of three years or longer standing in the Society.

Section 3. A candidate for student associate membership shall be at least 18 years old and shall be a bona fide student in a Science or Engineering course and shall be under 29 years of age. Election to student associate membership shall require recommendation by at least two active members of three years or longer standing in the Society. No student membership shall extend beyond the year of becoming 28 years old.

Section 4. A candidate for associate membership shall have received the Bachelor of Science (or of Engineering) degree, but not yet have completed the requirement of three years' experience, nor have exceeded the age of 28. Election to associate membership shall require recommendation by at least two active members of three years or longer standing in the Society.

ARTICLE III

Admission and Dismissal of Members:

Section 2. Application for admission after April 6, 1902, shall be made in writing in a form prescribed by the Board of Directors, and shall refer to at least two members. The application shall also state the present occupation of the applicant, and briefly in what capacity he is interested in the subject of electrochemistry.

Section 3. The Assistant Secretary shall submit to each Director the names and addresses of applicants and of their respective references, provided the applications are in due form and that the applicant has been favorably recommended by his references. The election to membership shall be by vote of the Board of Directors or of its Executive Committee. If a candidate receives one negative vote his application shall then be considered and voted upon at a duly called meeting of the Board of Directors. Two negative votes cast at this meeting shall exclude a candidate. The Board of Directors may refuse to elect a candidate who, in its opinion, is not qualified for membership. The names of those elected shall be announced to the Society. A candidate who has been duly elected shall be placed on the rolls and have all the rights and privileges of a member as soon as his entrance fee and dues for the current year have been paid.

ARTICLE IV

Dues:

Section 2. The annual dues shall be payable at the beginning of the calendar year, and notice thereof shall be mailed to each member before the end of the preceding year. If not paid before the first day of April, the delinquent member shall lose his right to vote or to receive the publications of the Society, until said dues are paid. Members will pay dues for, and receive the publications of, the year in which they are elected, but if elected after July first will pay one-half the yearly dues and receive one-half of the publications of that year. Those members elected within two months of the end of the calendar year may, at their option, pay for, and enter with, the next coming year.

---

* Incorporating revisions effective January 1, 1950.